International Journal of Neural Systems, Vol. 27, No. 2 (2017) 1650009 (24 pages)

DOI: 10.1142/S012906571650009X

World Scientific
www.worldscientific.com

Superlinear Summation of Information in Premotor Neuron Pairs

Fernando Montani
Iflysib, Conicet & Universidad Nacional de La Plata
59-789 La Plata, Argentina
fmontani@gmail.com, f.montani@fisica.unlp.edu.ar

Andriy Oliynyk
Section of Human Physiology
Department of Biomedical Sciences and Advanced Therapies
Faculty of Medicine, University of Ferrara
Via Fossato di Mortara 17/19, 44121 Ferrara, Italy

Luciano Fadiga
IIT@UNIFE Center for Translational Neurophysiology
Istituto Italiano di Tecnologia, Ferrara, Italy
Section of Human Physiology, University of Ferrara, Italy

Accepted 15 December 2015
Published Online 11 February 2016

Whether premotor/motor neurons encode information in terms of spiking frequency or by their relative time of firing, which may display synchronization, is still undetermined. To address this issue, we used an information theory approach to analyze neuronal responses recorded in the premotor (area F5) and primary motor (area F1) cortices of macaque monkeys under four different conditions of visual feedback during hand grasping. To evaluate the sensitivity of spike timing correlation between single neurons, we investigated the stimulus dependent synchronization in our population of pairs. We first investigated the degree of correlation of trial-to-trial fluctuations in response strength between neighboring neurons for each condition, and second estimated the stimulus dependent synchronization by means of an information theoretical approach. We compared the information conveyed by pairs of simultaneously recorded neurons with the sum of information provided by the respective individual cells. The information transmission across pairs of cells in the primary motor cortex seems largely independent, whereas information transmission across pairs of premotor neurons is summed superlinearly. The brain could take advantage of both the accuracy provided by the independency of F1 and the synergy allowed by the superlinear information population coding in F5, distinguishing thus the generalizing role of F5.

Keywords: Neural code; motor control; information theory; spike synchronization; neural networks; Cortex.

1. Introduction

The relationship between the spiking activity of neurons and the state of the surrounding world is of paramount importance for understanding brain functions. As the spiking activity across cortical neurons is not independent, one needs to understand how neurons work together to represent sensorimotor information by translating it into spike trains. In the most recent years it has become more and more clear that perceptual mechanisms do not rely only on sensory information. Indeed, brain functions such as arousal, attention, perceptual enhancement are the result of a dialogue between sensory and premotor-prefrontal centers. In this regard, object representation and grasping control mechanisms have been the focus of interest for many researchers (for a review see Refs. 1 and 2). Their endeavors have shown that grasping control mechanisms require the

synergistic activity of a visuomotor network comprising the anterior intraparietal area (AIP), and area F5 of the ventral premotor cortex (PMv)[3,4] to transform object representations into grasping motor commands, which are subject to further processing in the primary motor cortex (area F1).[5,6]

It has been generally assumed that the representation of movement and hand grasping parameters are mediated by the average firing rate in these areas.[7] However, the firing rate alone may be too simplistic for describing complex brain activity and has been repeatedly discussed.[8–10] *Spike and EEG synchronization between/across neurons* has received attention as a novel coding dimension, due to its prevalence in cortical networks and its possible functional relevance to perceptual binding and sensorimotor integration for conveying stimulus-specific information.[11–20] Nevertheless, no recent study has attempted to address the relationship between synchrony of motor/premotor neurons during hand grasping, with and without visual feedback on the hand action.

To gain a better understanding of this issue, we considered two different instances. First, we investigated how complex neuronal representations of visuomotor and motor information are constructed from the activities of individual neurons. Secondly, to quantify their effect, we investigated whether synchronized spiking activity of nearby neurons within the premotor and motor cortices may carry additional information about the stimuli.

The degree of synchronous activity in a spiking neuronal network is usually characterized by simple parameters such as cross-correlation.[21,22] Moreover, techniques based on the dynamic properties of the spiking neural network[23–26] such as chaos control, desynchronization, phase resetting,[27,28] network topology,[29] optimization spiking,[30] artificial spiking neuronal networks,[31,32] code specificity, population code, and reinforcement learning[33,34] are very useful for describing important features of neural systems. Importantly, the transmitted information in a spiking neural network can be encoded in the frequency of spiking (*rate encoding*) and/or in the timing of the spikes (*pulse encoding*).[35,36] Pulse encoding is more powerful than rate encoding in terms of the wide range of information that may be encoded by the same number of neurons.[36] In order to characterize a spiking neuronal network we should consider therefore the amount of information that could be encoded by rate and/or pulse encoding.[36–38] More specifically, the information that the ensemble of neurons conveys about external stimuli can be broken down into firing rate ('*rate encoding like information*') and correlation components ('*pulse encoding like information*').[38–42] Thus, a quantitative answer to how correlation affects coding, independently of how responses are decoded, could be provided by Information Theory.[38–40,43–45] In this study, we applied an information theory approach to investigate the neural code of hand grasping. To do so, we estimated the premotor and motor information conveyed by areas F5 and F1, recording neuronal responses during four different conditions in the premotor and motor cortices of two unanesthetized, partially restrained macaque monkeys (*Macaca fascicularis*). The conditions were: grasping in full light, grasping in darkness, and grasping in darkness but with brief illumination of their acting hand during two critical phases of grasping: hand preshaping and target touching.

To gain a quantitative understanding of how premotor cortical neurons might report different stimuli, cells were classified into different subsets according to their stimulus specificity. Subsequently, we conducted the information theory analysis in two stages. First, we compared the information conveyed by the individual neuronal responses of cells from F5 and F1, and second we investigated the correlation in stimulus encoding of the premotor and motor cortices, in a bid to explain the recently discovered functional difference between the two areas noted during the observation of meaningful phases of the monkey's hand grasping action.[5]

2. Materials and Methods

2.1. *Experimental procedures*

Experimental protocols were approved by the Veterinarian Animal Care and Use Committee of the University of Ferrara, by the Italian Ministry of Health, and complied with the European laws on the use of laboratory animals. The present study is based on the analysis of data acquired in previous monkey's experiments regarding the role of hand-related visual feedback during grasping execution.[5] Therefore, all preparatory steps, basic procedures,

grasping tasks, electrophysiological recordings, selection of neurons and dataset (including ethical authorizations, single- neuron activity during grasping tasks, intracortical microstimulation data, kinematic measurements, etc.) were the same as those described by Ref. 5. Briefly, single-unit activity was recorded from areas F5 and F1 in three hemispheres of two behaving monkeys (*Macaca fascicularis*). Monkeys MK1 and MK2 (one female and one male, weighing 5.7 and 4.9 kg, respectively) were trained to perform a grasping task while sitting on a primate chair. After training, recording chambers (diameter 30 mm, left and right hemispheres of MK1, and left hemisphere of MK2) and a head-restraining device were surgically implanted. After the necessary recovery, more than 500 units were recorded. From those units, we isolated 169 F5 stable and valid neurons (102 from both hemispheres of MK1 and 67 from the left hemisphere of MK2) and 128 F1 neurons (106 and 22 from the left hemispheres of MK1 and MK2, respectively). Among these units we found and analyzed 42 pairs of single neurons of area F5 and 36 pairs of area F1. Wavelet methodology can usually help to improve single unit isolation in primary motor cortex cells.[46] However, in this paper, we take advantage of techniques such as fuzzy logic that are powerful signal processing tools.[47] More specifically, all these neuron pairs were recorded simultaneously during grasping tasks by one single recording electrode and were then carefully selected by using the Fuzzy Spike Sorting technique (FSPS^{TM}, see Ref. 48 for more details). Our FSPS^{TM} algorithm provided us fast and robust *online* classification of single neuron activity during the experiment.[5]

The macaque performed a precision grip task under four different conditions: (1) Light (**L**): grasping executed with continuous vision of its hand movement. (2) Dark (**D**): grasping executed in the absence of any visual feedback on its hand movement. (3) PT-flash condition (**P**): grasping executed in the dark with instantaneous visual feedback before touching, during the handgrip-shaping phase. (4) T-flash condition (**T**): grasping executed in the dark with instantaneous visual feedback at hand–object contact. In all the conditions the target object was always kept visible by a dim back-illumination. Experimental conditions were presented in blocks of twelve trials and administered with the above temporal order in all sessions. The **L** condition was then repeated at the end of each session to confirm the stability of neuronal activity (**L2** condition).

The **P** condition correspond to the case in which grasping was executed in dark but with instantaneous visual feedback during the hand preshaping phase. During the flash conditions, the scene was briefly illuminated by a single 20 μs xenon light flash delivered when the hand crossed an infrared barrier at 10 cm in front of the apparatus (PT-flash) or when both the thumb and index finger touched two small metal contact sensors attached to the sides of the to-be-grasped handle (T-flash). The **T** condition, is similar to the PT-flash condition but with instantaneous visual feedback provided at hand-object contact. The time sequence of events during the grasping task and neuron recording are reported in the experimental setup of Ref. 5. See also Ref. 5 for a detailed description of the experimental tasks, instrumental methods and electrophysiological recordings involved.

2.2. *Spike sorting*

The isolation of single neurons from multispike recordings was performed off-line using FSPS^{TM} software, based on singular value decomposition of the data matrix containing the different spike waveforms, followed by Fuzzy C-mean cluster analysis of the principal components in multidimensional space.[48] The good quality of the discrimination was confirmed by evaluating single-unit interspike interval histograms and the main quantitative parameters of cluster quality, including L_{ratio} measures.[48,49] To investigate the synchronicity between pairs of neurons recorded from the same electrode, we used a methodology similar to the one used in Ref. 38. That is, we identified pairs of single neurons and then investigated the role of correlation in stimulus encoding by using an exact information theoretic method to quantify the information conveyed by different coding mechanisms.[38]

Figures 1 and 2 show two representative examples recorded from areas F1 and F5, respectively; the single neurons were determined using the FSPS^{TM} software.[48] In both cases the two neurons were recorded simultaneously during task execution with the same electrode.

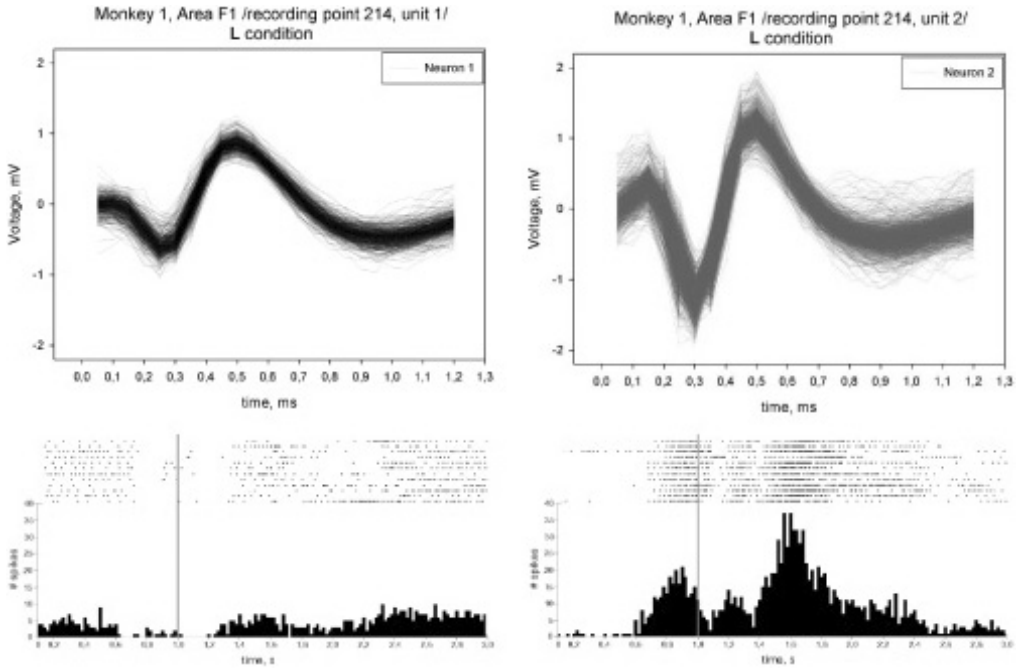

Fig. 1. Example of a typical single-neuron isolation performed using the FSPS^{TM} algorithm from Ref. 48. The upper part of the figure shows spike shapes for each of the detected clusters, while the lower part presents the corresponding histograms and rasters (multispike recordings of area F1).

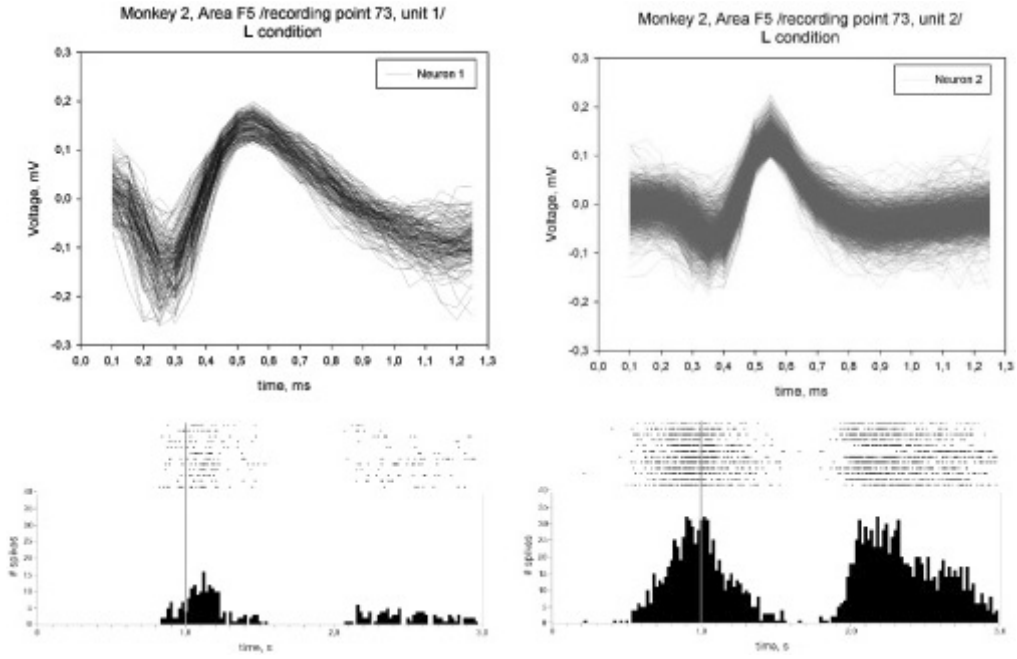

Fig. 2. Example of a typical single-neuron isolation performed using the FSPS^{TM} algorithm from Ref. 48. The upper part of the figure shows spike shapes for each of the detected clusters, while the lower part presents the corresponding histograms and rasters (multispike recordings of area F5).

2.3. *Information theory*

Shannon mutual information transmitted by the population response to the whole set of stimuli[38–40,50–52] was defined as

$$I(\mathrm{R};\mathrm{S}) = \left\langle \sum_{r\in R} P(r\,|\,s)\log_2\left(\frac{P(r\,|\,s)}{P(r)}\right)\right\rangle_s, \quad (1)$$

where the angular brackets indicate the average over different stimuli, $\langle A(s)\rangle_s \equiv \sum_{s\in S} P(s)A(s)$,

$P(s)$ is the probability that the stimulus s is present, $P(r\,|\,s)$ is the probability of observing the response r given stimulus s, and $P(r)$ is the probability of observing response r across all trials for any stimulus. It quantifies the reduction of uncertainty about the stimulus that can be gained from observation of a single trial of the neural response.[51–53] Then the probability $P(r\,|\,s)$ is determined experimentally by repeating each stimulus in exactly the same way on many trials, while recording the neuronal responses, and $P(r) = \langle P(r\,|\,s)\rangle_s$. Note that, in general, we quantify the responses in a discrete multidimensional array $r = r_1, \ldots, r_C$ of dimension C. For instance, the spike count response of a single cell would imply that $C = 1$, and r is the number of spikes emitted by this single cell in the response window in a given trial. However, if we consider the spike count response of a given pair of cells, then $C = 2$, and r_i is the number of spikes emitted by cell i (where $i = 1$ or 2) in the response window in a given trial. Note that in Eq. (1) the response window is defined by its duration, typically of a few milliseconds, and onset time.[38–40]

In Eq. (1), R and S denote the responses and stimulus sets, respectively.

Information breakdown decomposes the total mutual information into a sum of components related to the different ways in which correlations contribute to population coding,[38,40,52] such that

$$I(\mathrm{R};\mathrm{S}) = I_{\mathrm{lin}} + I_{\mathrm{sig-sim}} + I_{\mathrm{cor-ind}} + I_{\mathrm{cor-dep}}. \quad (2)$$

The first term of the information breakdown, I_{lin}, gives the total amount of information that would be conveyed if all the cells shared neither noise nor signal. The second term, i.e. $I_{\mathrm{sig-sim}}$, the signal similarity term, quantifies the amount of redundancy specifically due to signal correlation (i.e. similarity of the stimulus modulation of responses from individual cells). The term $I_{\mathrm{cor-ind}}$ quantifies the average level of correlation across the stimuli, and $I_{\mathrm{cor-dep}}$ quantifies the stimulus-dependent synchronization.

The information obtained if each cell were to convey independent information is defined as[38–40]:

$$I_{\mathrm{lin}} = \sum_c \sum_{r_c} \left\langle P(r_c\,|\,s)\log_2\left(\frac{P(r_c\,|\,s)}{P(r_c)}\right)\right\rangle_s, \quad (3)$$

where 'c' denotes the cell label, r_c is a vector describing the response of an individual cell. $P(r_c\,|\,s)$ is the probability of observing the response r_c given stimulus s for the individual cell 'c', and $P(r_c) = \langle P(r_c\,|\,s)\rangle_s$. The total impact of signal similarities on information transmission can be expressed as follows[38–40]:

$$I_{\mathrm{sig-sim}} = \frac{1}{\ln 2}\sum_r \left(\prod_c P(r_c)\right) \times\left\{(\nu(r) + (1+\nu(r))\cdot \ln\frac{1}{1+\nu(r)}\right\}. \quad (4)$$

In terms of information breakdown, the total amount of information attributable to the correlated activity of the overall neural coding is provided by $I_{\mathrm{cor}} = I_{\mathrm{cor-dep}} + I_{\mathrm{cor-ind}}$, where each terms reads as[38–40]:

$$I_{\mathrm{cor-dep}} = \sum_r \left\langle P_{\mathrm{ind}}(r\,|\,s)(1+\gamma(r\,|\,s)) \times \log_2 \frac{\langle P_{\mathrm{ind}}(r\,|\,s')\rangle_{s'}(1+\gamma(r\,|\,s))}{\langle P_{\mathrm{ind}}(r\,|\,s')(1+\gamma(r\,|\,s'))\rangle_{s'}}\right\rangle_s \quad (5)$$

and

$$I_{\mathrm{cor-ind}} = \sum_r \langle P_{\mathrm{ind}}(r\,|\,s)\gamma(r\,|\,s)\rangle_s \log_2\frac{1}{1+\nu(r)}. \quad (6)$$

Note that in the previous Eqs. (4)–(6) the noise correlation$\gamma(r\,|\,s)$ is defined as[38–40]:

$$\gamma(r\,|\,s) = \begin{cases} \dfrac{P(r\,|\,s)}{P_{\mathrm{ind}}(r\,|\,s)} - 1 & \text{if } P_{\mathrm{ind}}(r\,|\,s) \neq 0 \\ 0 & \text{Otherwise} \end{cases} \quad (7)$$

and the signal correlation coefficient $\nu(r)$ as[38–40]:

$$\nu(r) = \begin{cases} \dfrac{P_{\mathrm{ind}}(r)}{\prod_c P(r_c)} - 1 & \text{if } \left(\prod_c P(r_c)\right) \neq 0 \\ 0 & \text{Otherwise} \end{cases}, \quad (8)$$

where $\nu(r)$ quantifies how similar across stimuli the response probabilities of the individual cells that

form the population are and r_c is a vector describing the response of an individual cell ('c' denotes the cell label). $P_{\text{ind}}(r \mid s) = \prod_{c=1}^{C} P(r_c \mid s)$ is the distribution one would derive in absence of knowledge of correlations, and $P_{\text{ind}}(r) = \langle P_{\text{ind}}(r \mid s) \rangle_{s.}$.

In Appendix A, we provide a visual explanation of how the total mutual information is separated into components reflecting the contributions of individual coding mechanisms.

Neurophysiological experiments can only convey a finite number of trials, and therefore the true stimulus-response probabilities cannot be estimated with precision. The estimated probabilities fluctuate around their true values, and should then be corrected for bias, since this can lead to serious misinterpretations of neural coding data.[37,38,52,54] It is also important to point out that due to the small number of trials (12) it was crucial to use an effective sampling procedure. To correct for bias in the information calculations, we used three equipopulated response bins with fixed time window lengths $T = 100$ ms. That is to say, in order to facilitate the sampling of its probability, we discretized the response space by binning each time window of $T = 100$ ms into $R = 3$ equipopulated bins. To correct for sampling bias, we used a quadratic extrapolation procedure (QE, see Ref. 54) to estimate and subtract out the bias of each information quantity. For the current analysis, we found that the QE method (QE see Ref. 54) was the most stable, as the Panzeri–Treves[55] method used to remove sample-size-dependent bias from entropy estimations does not perform well for such a number of trials when the binning does not remain constant across the ensemble.

The pair-wise information $I(r_1 r_2; S)$ conveyed by joint observation of two cells was also estimated using the "shuffling procedure" described in Refs. 52 and 56, which greatly reduces the bias of multidimensional information estimates (I_{sh}). The performance of the "shuffling procedure" on realistically simulated neural spike trains has previously been reported in detail by other authors (see Refs. 38, 52 and 56). We chose $R = 3$ (number of equipopulated bins) because it was the largest number that consistently led to robust unbiased results under the sampling conditions of our experiment.

In the following, we describe how to assess noise correlations from the cross-correlograms (CCGs). When a stimulus is shown repeatedly, trial-to-trial fluctuations in response strength are correlated between neighboring cortical neurons. This correlation is typically characterized using the noise correlation r_{noise}. Furthermore, the timing of action potentials between nearby neurons is also often correlated or synchronized, as is usually shown by a peak in the spike train CCG (see for instance Refs. 22, 57–59). In this paper, we use different metrics to characterize correlations: the (shift-predictor-corrected) spike train CCG (see Ref. 58), noise correlation r_{noise},[22] and the information breakdown method.[38–40] All these concept can be joined together investigating how information is encoded by neural populations, and in particular Eq. (5) quantifies the stimulus dependent synchronization across pairs of neurons.

The average noise correlations r_{noise} were estimated across trials, and for each of the four stimuli, using the approach developed by Bair and Zohari.[59] This approach is based on the fact that r_{noise} can be rewritten in a form that is based solely on the areas under the spike train CCG and autocorrelograms (ACGs), as proposed in Ref. 59, such that

$$r_{\text{noise}} = \frac{\text{Area under CCG}}{\sqrt{\text{Area under ACG}_1 \times \text{Area under ACG}_2}}. \tag{9}$$

To compute the CCGs, the spike train of each cell is represented as a binary time series with 1 ms resolution, such that: $x_j^i(t) = 1$ if in trial i, neuron j fired an action potential during the tth millisecond, otherwise, $x_j^i(t) = 0$. ACG_1 and ACG_2 denote the spike train ACGs for each cell.[59] CCGs were computed as follows:

$$\text{CCG}(\tau) = \frac{\frac{1}{M} \sum_{i=1}^{M} \sum_{t=1}^{N} x_1^i(t) x_2^i(t+\tau)}{\theta(\tau)\sqrt{\lambda_1 \lambda_2}}, \tag{10}$$

where M is the number of trials, N is the number of bins in the trial, x_1^i and x_2^i are the spike trains of neurons 1 and 2 in trial i, τ is the time lag, and λ_1 and λ_2 are the mean firing rates of the two cells. $\theta(\tau)$ is the following triangular function: $\theta(\tau) = T - |\tau|$, where T is the trial duration in seconds. This function corrects for the degree of overlap of the two spike trains for each time lag (i.e. there are T opportunities for simultaneous events in a trial of length T, but only $T - 1$ opportunities for coincidences at time lags of 1 ms, etc.). Note that for ACGs estimations the lower indices of the neurons in Eq. (10) are considered the same.

All CCGs were corrected for correlation induced by the stimulus, subtracting a shift predictor calculated from trials 1 to $n-1$, with an offset of one trial. Specifically, the shift predictor was calculated as

$$\mathrm{SHIFT}(\tau) = \frac{1}{M-1} \sum_{i=1}^{M-1} \sum_{t=1}^{N} x_1^i(t) x_2^{i+1}(t+\tau). \quad (11)$$

However, CCGs only account for near-synchronous spikes. That is, they do not account for correlations that occur on longer timescales or among patterns of spikes. For instance, the firing rate can alter the shape of CCGs, making it difficult to separate information carried by firing rates from information carried by correlations. The dependence between responses and stimuli can take a number of forms: firing rate dependence, pair-wise correlation dependence, and so on.[38–40]

Information theory approaches have the unique advantage of capturing all nonlinear dependencies of any statistical order that may be present in the data. If synergistic or redundant interactions between cells are observed, the information components can reveal the mechanisms through which they arise. Likewise, spike correlations can be estimated using the information breakdown framework,[38–40] in which the total level of correlation quantifies the total amount of information resulting from the correlated activity on the overall neural coding. As we mentioned above, this term is further resolved in two components $I_{\mathrm{cor}} = I_{\mathrm{cor-ind}} + I_{\mathrm{cor-dep}}$, which capture the average level of correlation $I_{\mathrm{cor-ind}}$ (see Eq. (6)), and the stimulus-dependent synchronization component $I_{\mathrm{cor-dep}}$(see Eq. (5)). In this way, information component breakdown methods allow us to quantify the effect of such dependencies on the mutual information, and thereby assess the different ways in which the correlations contribute to the neural code.[38–40]

3. Results

We estimated first the average mutual information as calculated from the individual responses of 128 single neurons in F1 and 169 single neurons in F5. All neurons were similar to the "nonobject type" visual-motor neurons previously described in area AIP.[60] These neurons, whose discharge properties can be considered as intermediate between the motor and the visual-motor classes, have been thought to respond to handgrip selectivity or to a combined view of handgrip and object. They did not respond to object presentation, as shown by the naturalistic testing and by the absence of any response to the mere observation of the to-be-grasped object during the formal testing.[5] In fact, in the naturalistic test preceding the experiment, neurons showing activity related to the observation of objects and, in particular, of small solid cubes matching the shape of the door handle in the experimental apparatus were not included in the study; in addition, recorded neurons did not show any visual response to the sight of the door handle, after removal of the overlying external door by the experimenter, at the beginning of each trial. To investigate the stimulus-dependent synchrony of nearby cortical neurons in the premotor and motor areas on the neural coding of grasping, we used the information breakdown approach, specifically the information components method.[38–40]

3.1. *Linear information: Single-cell analysis*

Figures 3 and 4 show representative examples of single-cell firing patterns within F5 and F1 under the four different stimulus conditions: **L**, **D**, **P** (PT-flash) and **T** (T-flash), previously described in Ref. 5. This is representative of the overall behavior of the population, although the single cells within F1 are generally more specific than those in F5. Indeed, F5 neurons are sensitive to the observation of meaningful phases of the grasping action, while F1 neurons are more specific to motor task.[5,61,62] To undergo further analysis, we also considered different subsets of neurons that fulfilled the following conditions: (i) $\mathbf{L} > \mathbf{D}$, (ii) $\mathbf{D} > \mathbf{L}$, (iii) $\mathbf{P} > \mathbf{D}$, (iv) $\mathbf{D} > \mathbf{P}$, (v) $\mathbf{P} > \mathbf{L}$, and (vi) $\mathbf{L} > \mathbf{P}$. The subsets were defined by splitting the 250 ms before grasping (object touch with both grasping fingers) into five bins of 50 ms. The notation 'greater than' (">") indicates a set of neurons that under a given stimulus condition showed a significant increase in firing rate than other given stimulus condition ($p < 0.05$, two sample t-test). That is, we considered different subgroups of cells that satisfied each of the mentioned constraints (i)–(vi) for the five bins of 50 ms.

We then examined the population coding for grasping in the premotor and motor cortices by quantifying responses as the number of spikes fired by each cell within time window T (typically 100 ms,

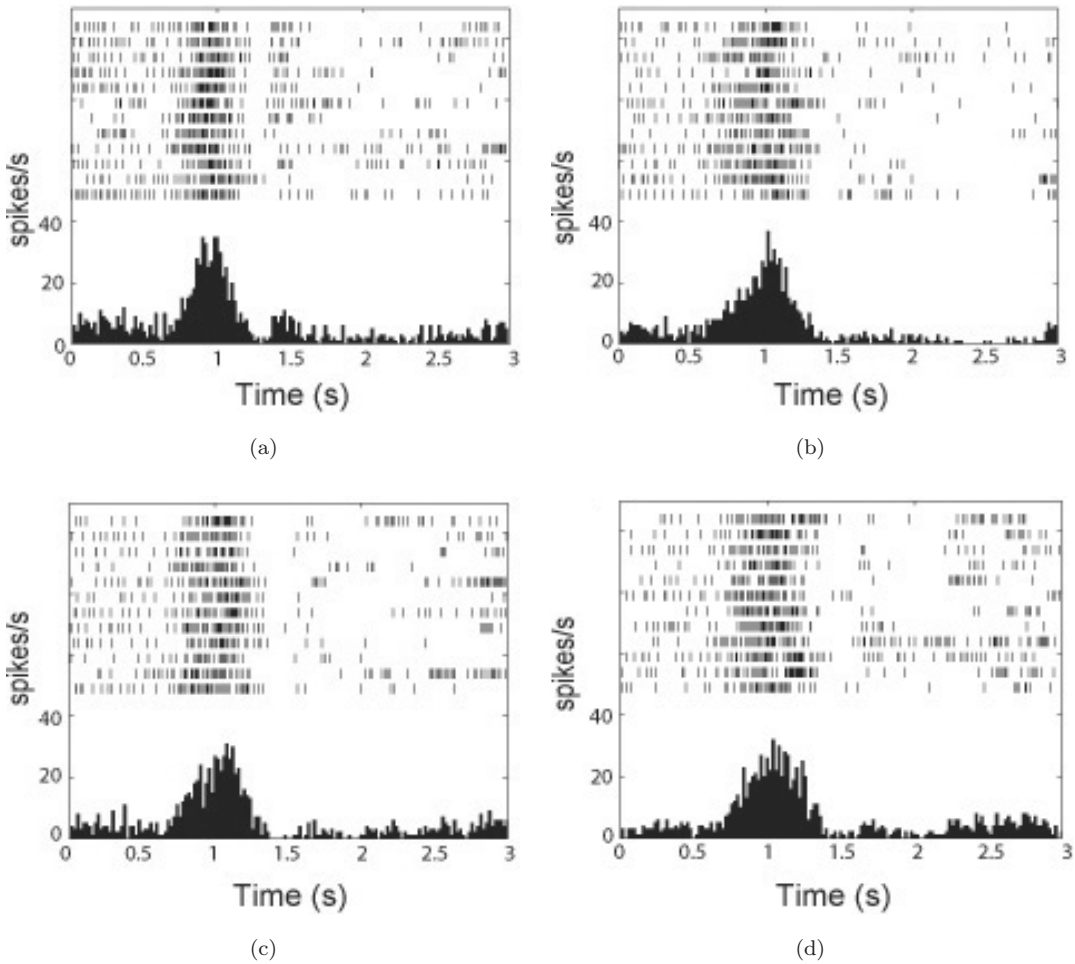

Fig. 3. Example of grasping-related activity motor-dominant neuron in the area F5 under four different stimulus conditions: (a) Light (**L**), (b) Dark (**D**), (c) PT-flash (**P**), and (d) T-flash (**T**). *Note*: Rasters and histograms are aligned with the grasp of the handle marked by the vertical line at 1 s.

$R = 3$). We calculated the average information conveyed by the single-cell population that responded to the stimulus. More specifically, average mutual information values estimated using Eq. (1) from the individual neuronal responses (I_{F5} for F5 and I_{F1} for F1) were obtained for the entire population and for the different subsets of cells (i)–(vi). To study which stimulus feature or what combinations of features are encoded in the neuronal response we perform these mutual information estimations for each of the different set of stimuli, made up of all the possible combinations of the four distinct conditions (**L**, **D**, **P**, and **T**). These set of stimuli combinations are given by **DLPT, DLT, DLP, DL, TP, LT, DP, DT, LP, LTP**, and **DTP.** We consider the whole population of cells, and the subsets of cells (i)–(vi). Figure 5(a) shows the mutual information for the **DLPT** combination considering the entire time range of analysis (3 s). Figure 5(b) shows the average mutual information between 0.5 and 1.5 s for the other 10 combinations of stimuli (**DLT, DLP, DL, TP, LT, DP, DT, LP, LTP**, and **DTP)**. With respect to the whole population, it is evident that the information conveyed by F1 is larger than that conveyed by F5.

Visual information on the performed movement is transformed from an extrinsic reference framework (F5) that defines the spatial position of the hand with respect to the object to an intrinsic framework (F1) based on muscle and joint space to generate accurate grasping.[5] F5 is implicated in an early phase, the control of distal movements, while F1 in intrinsic phase of action. Thus, F5 is involved in a level of processing hierarchically higher than F1, and

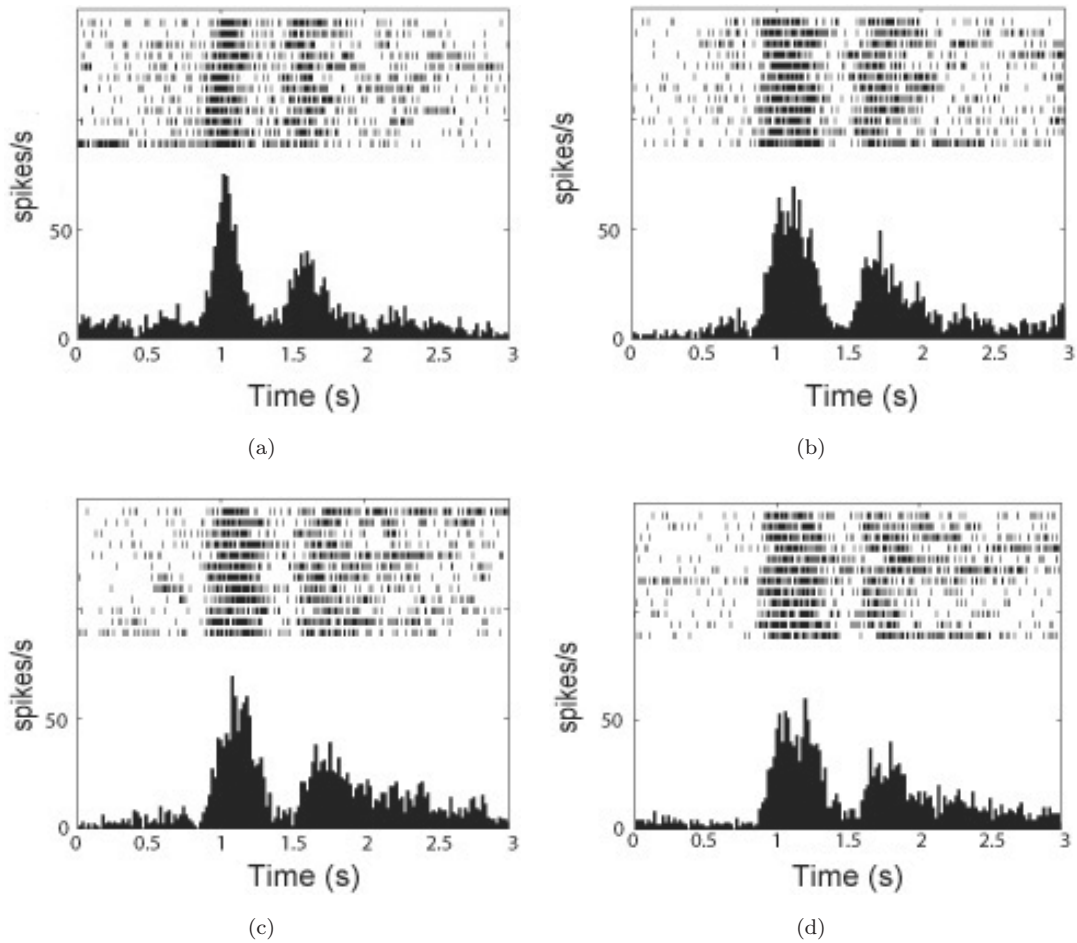

Fig. 4. Example of grasping-related motor neuron in the area F5 under four different stimulus conditions: (a) Light (**L**), (b) Dark (**D**), (c) PT-flash (**P**), and (d) T-flash (**T**). *Note*: Rasters and histograms are aligned with the grasp of the handle marked by the vertical line at 1 s.

the previous result seems counterintuitive. However, it could be that possible differences in neuronal activity are caused by changes in kinematics between light and dark conditions. For this reason, in addition to the traditional **L** versus **D**, we also considered and compared two further conditions, **P** and **T**, which did not show any kinematic difference with respect to **D**, thereby ensuring that any effect of the dark on arm/hand kinematics was taken into account. Indeed, the combination of **P** and **T** exhibits very different behavior, with F5 becoming more informative than F1. Figure 5(c) shows the average mutual information between 1.5 and 2.5 s using the same stimulus combinations as in Fig. 5(b). We can see that for all the stimulus combinations that do not feature condition **L** (i.e. **PT**, **DTP**, **DT**, and **DTP**) the information in F1 is less than the information in F5. This effect is very strong and enables us to easily distinguish cells belonging to F5 from those belonging to F1. Thus, the comparison of mutual information values of stimulus combinations with and without the **L** condition provides a hitherto unknown method of identifying a population ensemble within F1 (or within F5). Moreover, it shows that visual information conveyed by the brief illumination of the monkey's hand in action (**P** and **T** conditions) has a greater effect on F5 than on F1 when the whole population of neurons is considered. A possible explanation for this difference could be the distinctive contribution of premotor area F5 to the motor-relevant visual feedback (as suggested by the recent neurophysiological studies of Refs. 5, 61 and 62). Hence, information theory allows us to redefine the problem of cell classification, to identify which stimulus

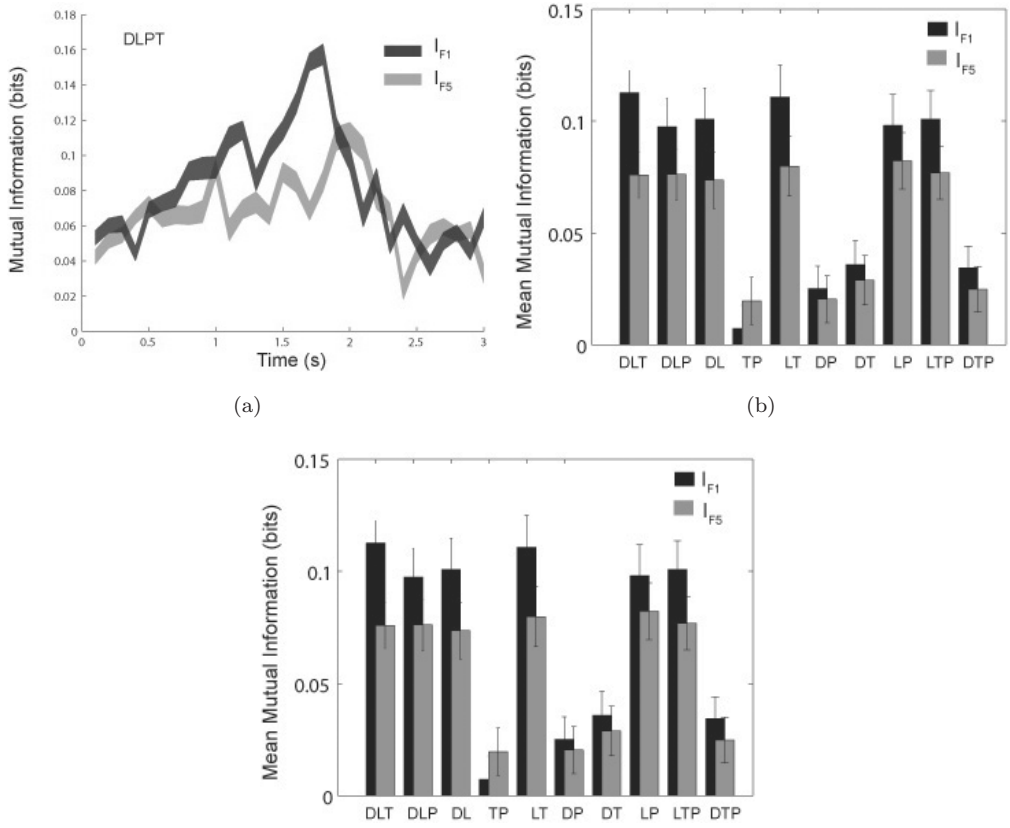

Fig. 5. Average mutual information conveyed by area F5 and area F1 during hand grasping for different stimulus combinations: single-cell analysis. (a) The average mutual information for the four stimulus combinations Dark/Light/Pre-touch/Flash-Touch-Flash (**DLPT**) for the entire time range of analysis (3 s). We considered 169 single neurons in F5 and 128 single neurons in F1. (b) The average mutual information between 0.5 and 1.5 s for the other 10 possible stimulus combinations (**DLT, DLP, DL, TP, LT, DPT, DT, LP, LTP**, and **DTP**). Overall, the average information conveyed by the neurons in F1 is greater than the information conveyed by F5. However, note in panel B that with the combination of stimuli **P** and **T,** the reverse is true, i.e. F5 is more informative than F1. (c) The average mutual information conveyed between 1.5 and 2.5 s, using the same stimulus combinations as in panel B. Note that for all the stimulus combinations without the **L** condition (i.e. **PT, DTP, DT**, and **DTP**) the information transmitted in F1 is smaller than that in F5. Analyzing stimulus combinations without the **L** condition in comparison with those with **L** condition can help us to "identify" a population ensemble within F1 (or within F5).

combinations are most significant for each area, without imposing a metric between neuronal responses and stimulus variables. The pattern seen in Fig. 5(a) applies generally across the dataset.

This behavior remained substantially uniform across the subpopulation of cells that met the conditions (i) and (ii), as shown in Figs. 6(a)–6(d). Figures 6(e) and 6(f) show the mean of the single-cell information values that satisfied the condition (iii). All these estimations were performed using Eq. (1). For any time window before object touching (1 s) smaller than 200 ms, the Kolmogorov–Smirnov tests rejected the hypothesis that the distributions of I_{F1} and I_{F5} are the same (**DLPT** stimulus combination). Furthermore, these particular groups of cells exhibited higher information values for F5 than for F1 at any time shorter than 1 s. After 1 s, the behavior is inverted, and F1 is shown to be more informative than F5. Hence, this particular subset of cells appears to exhibit specific stimulus adaptation during the reach-to-grasp task. Figures 7(a) and 7(b) show the mean of the single-cell information values that satisfied the condition (v). This particular subset of cells also exhibits information values higher for F5 than for F1 over short time ranges at the beginning of the experiment. In contrast to our

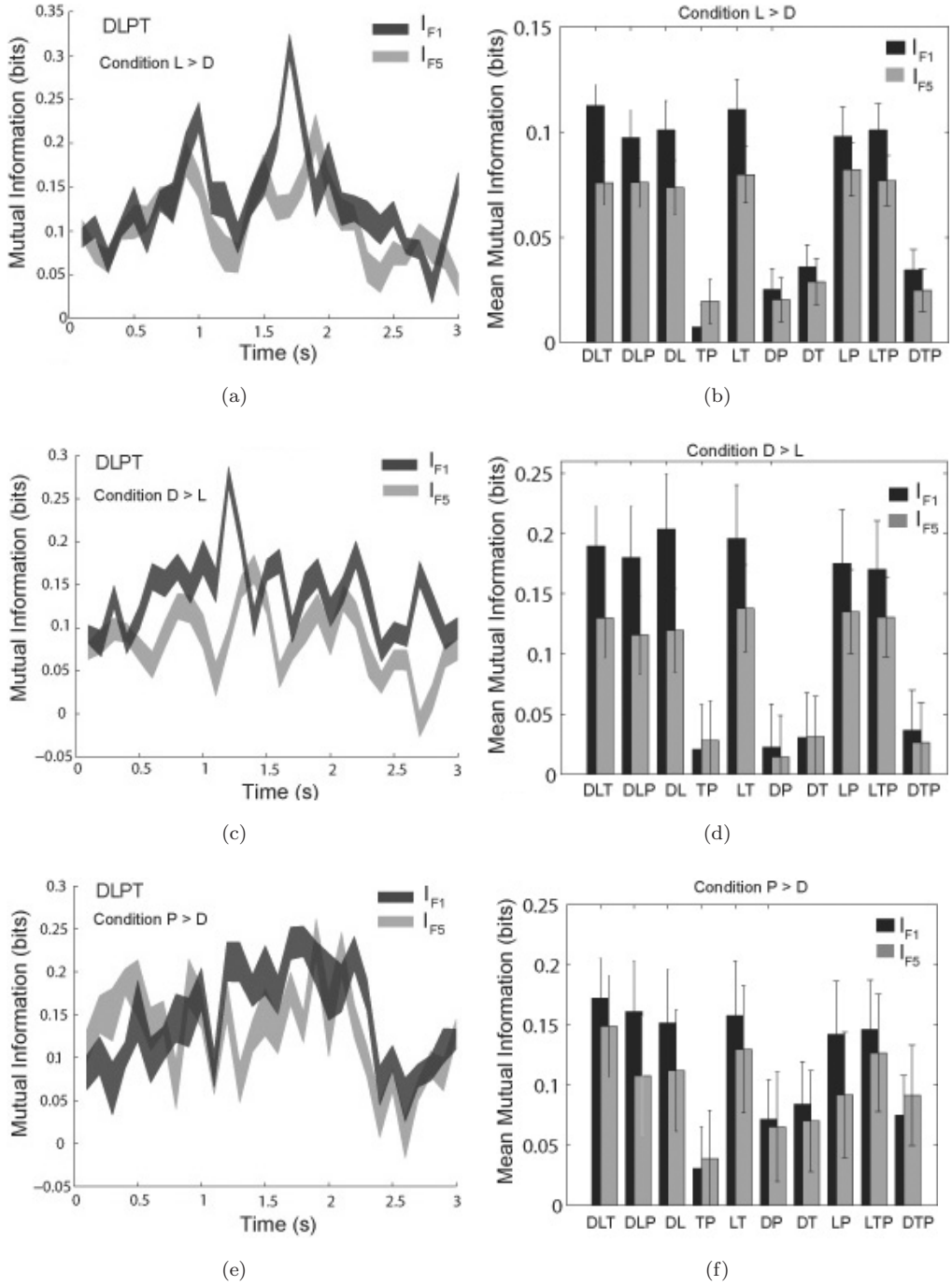

Fig. 6. The classification of light-modulated neurons into different groups according to their response to a stimulus. The classification was performed choosing a time of 250 ms before the time of grasping (1 s), with five bins of 50 ms. (a) Average information conveyed by the single-cell population that met the condition **L > D** (**DLPT** stimulus combination). (b) Average mutual information between 0.5 and 1.5 s (**DLT**, **DLP**, **DL**, **TP**, **LT**, **DPT**, **DT**, **LP**, **LTP**, and **DTP**) that met the condition **L > D**. (c) Average information from the single-cell population that met the condition **D > L** (**DLPT** stimulus combination). (d) Average mutual information between 0.5 and 1.5 s (**DLT**, **DLP**, **DL, TP**, **LT**, **DPT**, **DT**, **LP**, **LTP,** and **DTP**) that met the condition **D > L**. (e) Average information from the single-cell population that met the condition **P > D** (**DLPT** stimulus combination). (f) Average mutual information between 0.5 and 1.5 s (**DLT**, **DLP**, **DL, TP**, **LT**, **DPT**, **DT**, **LP**, **LTP**, and **DTP**) that met the condition **P > D**. Note that these particular groups of cells exhibited higher information values for F5 than for F1 at times shorter than 1 s. Thereafter, the behavior was inverted.

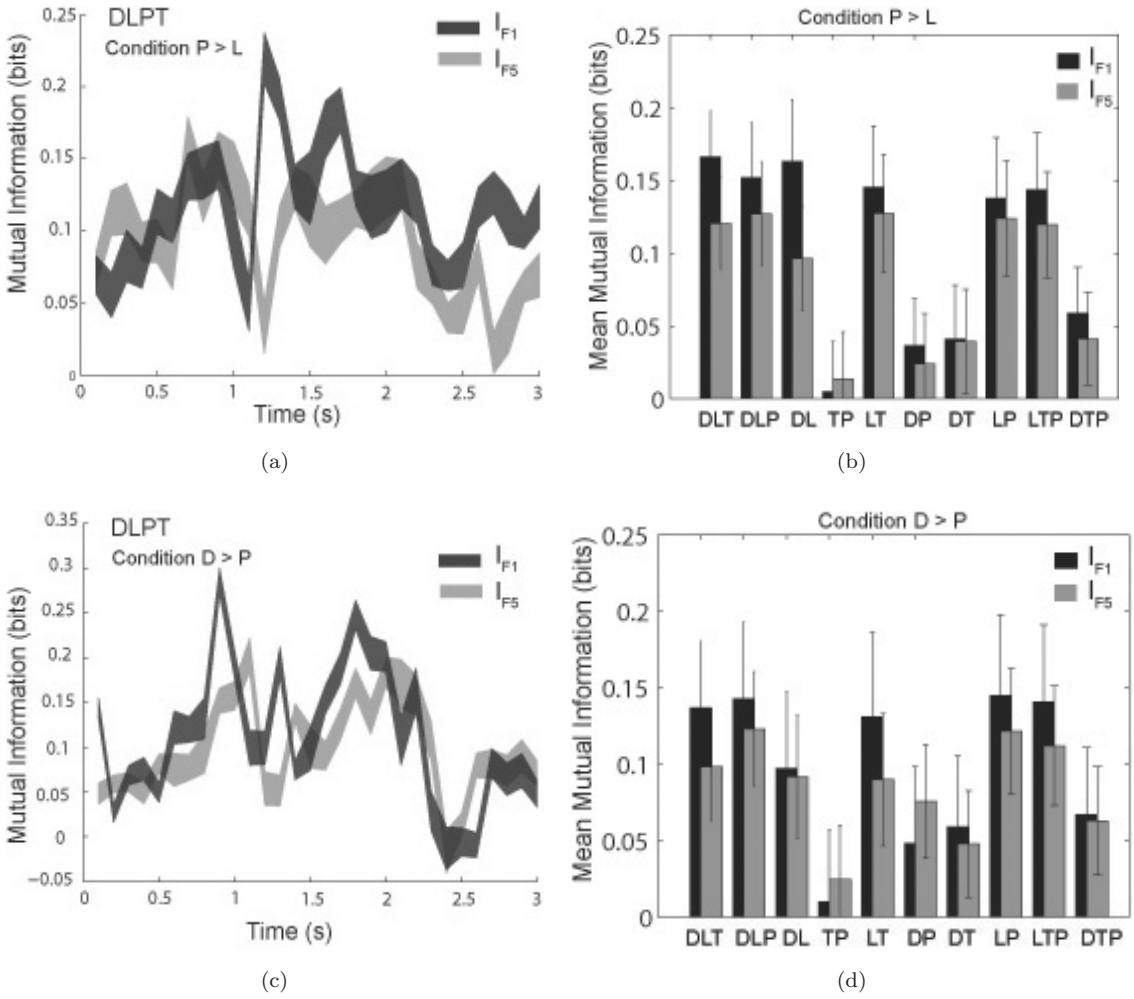

(a) (b) (c) (d)

Fig. 7. The classification of flash-modulated neurons into different groups according to their response to a stimulus. The classification was performed choosing a time of 250 ms before the time of grasping (1 s), with five bins of 50 ms. (a) Average information from the single-cell population that met the condition P > L (DLPT stimulus combination). (b) Average mutual information between 0.5 and 1.5 s (DLT, DLP, DL, TP, LT, DPT, DT, LP, LTP, and DTP) that met the condition P > L. (c) Average information from the single-cell population that met the condition D > P (DLPT stimulus combination). (d) Average mutual information between 0.5 and 1.5 s (DLT, DLP, DL, TP, LT, DPT, DT, LP, LTP, and DTP) that met the condition D > P. (e) Average information conveyed by the single-cell population that met the condition L > P (DLPT stimulus combination). (f) Average information between 0.5 and 1.5 s (DLT, DLP, DL, TP, LT, DPT, DT, LP, LTP, and DTP) meeting the condition L > P. Overall, the average information conveyed by F1 is greater than the information conveyed by F5. Note that in panel B, D and F, in the case of PT the information conveyed by F5 is greater than the information available in F1.

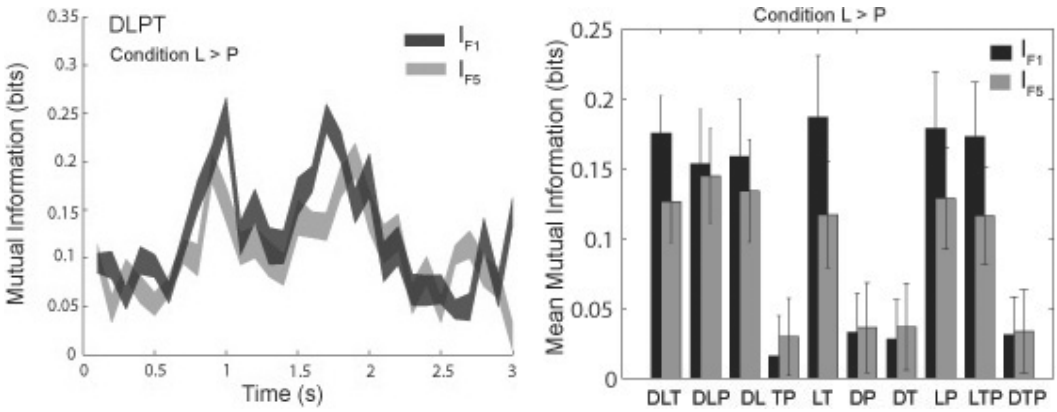

(e) (f)

Fig. 7. (*Continued*)

findings in Fig. 6(e), the Kolmogorov–Smirnov tests cannot reject the hypothesis that the distributions are equal. Figures 7(c)–7(f) show the mean of the single-cell information values for the cell subsets satisfying the conditions (iv) and (vi), respectively. In general, when considering subsets (i), (ii), (iv), (v), and (vi), the information conveyed by the average information of F1 is greater than the information conveyed by F5. These values were obtained using Eq. (1). In summary, our findings show that a simple comparison of mutual information values between stimulus combinations with or without the **L** condition enables us to readily classify cells as belonging to either F5 or F1. We also found that a particular subset of cells, which has **P**-stimulus spike responses larger than in the **D** condition, exhibits a specific stimulus adaptation through the task execution.

3.2. *Pairwise correlations in grasp coding within the motor and premotor areas*

In the previous section we showed that, for linear coding, F1 is more informative than F5 under full vision (**L**) conditions. Considering the fact that this could reflect finger posture adjustments derived from proprioceptive feedback for accurate hand preshaping in dark conditions (**D**, **P**, and **T**) this is not surprising if we think in terms of a multilayer network, as F1 is closer to the output than F5. Further down the pathway, information from the primary motor cortex (F1) is conveyed to cells in the spinal cord via the corticospinal tract, a primary neural substrate for independent finger movements.[63,64] Our single-cell analysis also shows how different areas could process information generated by different stimulus combinations. Thus, comparing mutual information values of stimulus combinations with and without the **L** condition provides us with a method to classify cells as belonging to either F1 or F5.

However, this does not enable us to resolve the issue of synchronized neural coding. It is well established that the timing of action potentials of nearby neurons is often correlated or synchronized.[38–40] It is, therefore, important to focus on how pairs of cells with common inputs and similar receptive fields might be affected by spike synchrony. It is unclear, however, how the synchrony between single neurons within F5 and F1 is affected by basic stimulus manipulations such as **L**, **D**, **P**, and **T**. Characterizing the correlation and its stimulus dependence is important for understanding the computations that can be performed by a neuronal population. Additionally, interactions between neurons may encode combinations of parameters: von der Malsburg,[65] for example, suggested that the binding of different features belonging to one object is represented by synchronous neural discharges. Correlations between neurons encoding distinct parameters occur in specific parameter combinations, in which stimulus/behavioral requirements match the properties of the neurons. Furthermore, a particularly important theoretical reason to study correlations is that the capacity of a population rate code to encode information can depend on the magnitude of correlated variability, its relationship to the signal similarity between neurons, and its dependence on stimulus drive.[66]

3.2.1. *Spike train CCG*

Figures 8(a) and 8(b) show the peristimulus histograms (PSTHs) for two typical pairs of cells in F5 and F1, respectively, while Figs. 8(c) and 8(d) show the CCGs for the same pairs of cells, estimated using Eq. (10). The correlation is characterized using a (shift-predictor-corrected) spike train CCG (see Ref. 59). We presented four stimuli that drove each cell through the firing rates, which resulted in a substantial modulation in the height of the central peak of the neuron spike-train CCG. At a particular stimulus that drives both neurons moderately well, a fraction of the spikes fired by each neuron tend to be synchronized with millisecond temporal precision. This result can be verified for both F5 and F1 neuron pairs, as shown in Figs. 8(c) and 8(d). This stimulus dependence of synchrony arises despite correcting for the basic rate dependence of the CCG. Figures 9(a)–9(h) show the average noise correlation over the entire population of pairs, r_{noise} as in Eq. (9), within F1 and F5. The data presented in Fig. 9 show the histograms for r_{noise} in our population of pairs, in order to illustrate the relationship between spike counts and noise correlation.The average noise correlations for F5 are 0.26 ± 0.02 (L), 0.37 ± 0.02 (D), 0.43 ± 0.02 (P), and 0.29 ± 0.02 (T). In contrast the average noise correlations of F1 are 0.1 ± 0.03 (L), 0.18 ± 0.03 (D), 0.17 ± 0.03 (P), and 0.245 ± 0.03 (T). The r_{noise} estimation was performed by taking a time lag T of 200 ms before and after the time of touching (1 s). The distributions are significantly different; the Kolmogorov–Smirnov tests rejected the hypothesis that the distributions are the same. Note therefore that both areas F5 and F1 show a significant amount of noise correlation and stimulus dependence. However, the average signal correlation values, r_{signal}, for the entire population of pairs (estimated as the Pearson correlation between the mean responses of each cell to each stimulus) were quite low: 0.1560 ± 0.0346 for F5 and 0.260 ± 0.0298 for F1.

3.2.2. *Information component breakdown*

Figures 10(a)–10(c) show the information fraction considered for time windows of ± 200 ms, ± 100 ms, and ± 50 ms before and after the 1st second (considering 42 pairs of F5 and 36 pairs of F1). We estimated the information fractions by estimating the information components given Eqs. (3)–(6) that were divided by the information of the ensemble obtained using Eq. (1). Figures 11(a) and 11(b) show the information values in bits, estimated using Eqs. (1)–(6). The picture shown by the entire population of pairs in F5 is that of a very significant amount of synergy: with time windows of ± 200 ms, ± 100 ms, and ± 50 ms (before and after the 1st second), the ensemble population code, $I_{\text{population}}$, outperforms the mean of single-cell information values, I_{lin}, by 32.0%, 46.6%, and 58.4% on average, respectively. The linear term in the case of F5, I_{lin}, accounts only for 68.0%, 53.4%, and 41.6% of the total ensemble information, and the stimulus component correlation, $I_{\text{cor}-\text{dep}}$, corresponds to 45.0%, 43.5%, 43.9% of the total information, respectively, for the time windows of ± 200 ms, ± 100 ms and ± 50 ms.

In contrast, when considering F1 population, the amount of synergy is about half of the value obtained for F5. That is, the population ensemble performs, on average, 14.45% and 26.31% better than the sum of single-cell contributions, respectively, for ± 200 ms and ± 100 ms (see Figs. 10(a) and 10(b)).

When considering F5 the ensemble information, $I_{\text{population}}$, is much higher than the sum of the single-cell information values (I_{lin}) for a wide range of time windows ± 200 ms, ± 100 ms, and ± 50 ms. The maximum difference we observed between F5 and F1 was a double amount of synergy for F5 at 200 ms and ± 100 ms, tailing off sharply at 50 ms, a point at which synergy values became similar (Fig. 10(c)). Thus, information across pairs of cells in F1 is roughly independent, whereas information across pairs of cells in the premotor cortex area F5 is summed superlinearly.

To test the robustness of our previous result, we consider a Poisson simulation of uncorrelated neurons that have exactly the same mean rates to each stimulus as the neuronal pair under consideration, but no noise correlations and the same number trials for each of the four experimental conditions. Correlations that manifest as covariation of the trial-by-trial fluctuation around the mean response are named "noise correlations".[37,62] On the other hand, correlations in response profiles of an individual signal across different stimuli are called "signal correlation"[39,67] because they are entirely attributable to stimulus selectivity. $P(\mathbf{r} \mid \mathbf{s})$ is the true distribution of stimuli given responses, and $P_{\text{ind}}(\mathbf{r} \mid \mathbf{s})$ is the distribution one would derive in the absence of knowledge

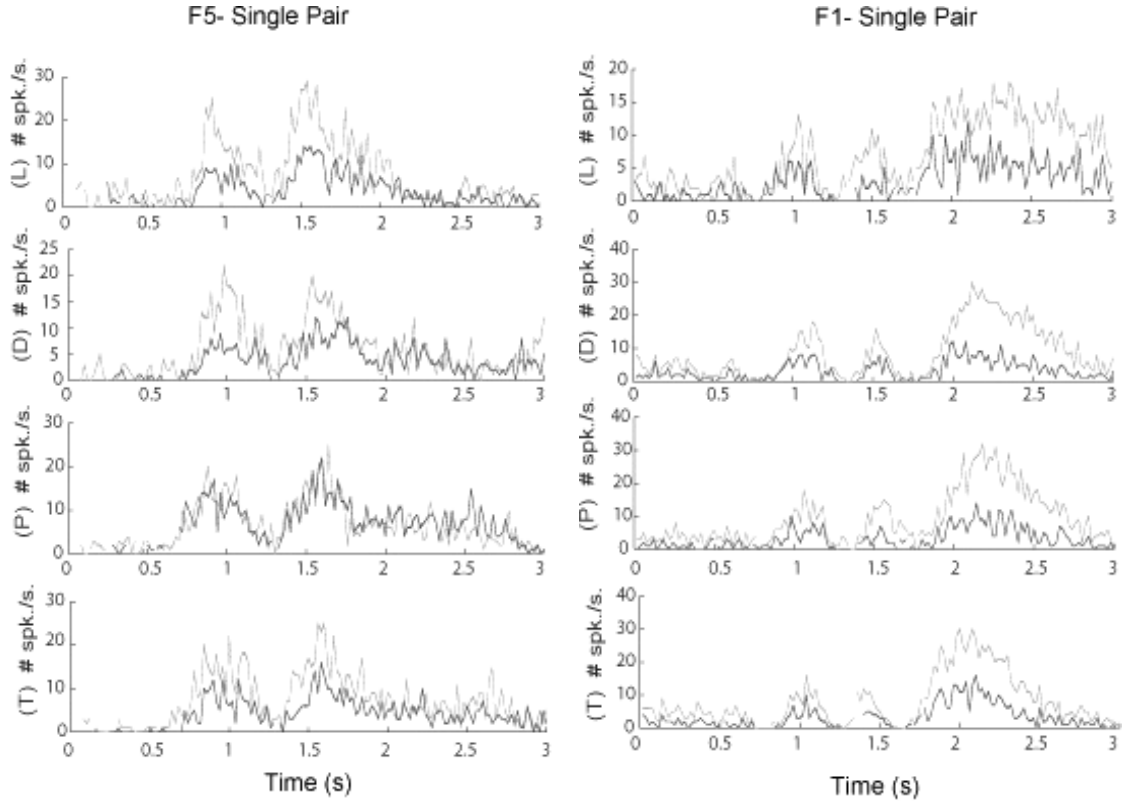

(a) (b)

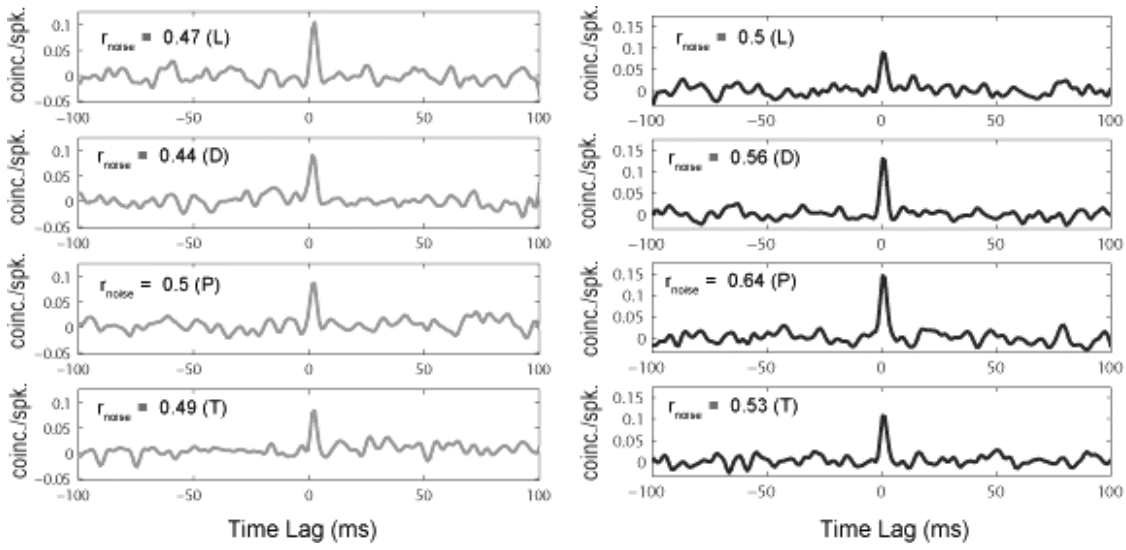

(c) (d)

Fig. 8. Interaction between neuronal pairs in premotor and motor cortices. (a) and (c) correspond to the PSTHs and CCG for the responses of a given pair of cells in F5. (b) and (d) correspond to the PSTH and CCG of a given pair of cells in F1. The cross-correlation was estimated for the four stimulus conditions. The corresponding r_{noise} values are indicated in each panel. CCGs for the pair above show that fine-timescale synchronization is induced for stimuli that drive both cells relatively well.

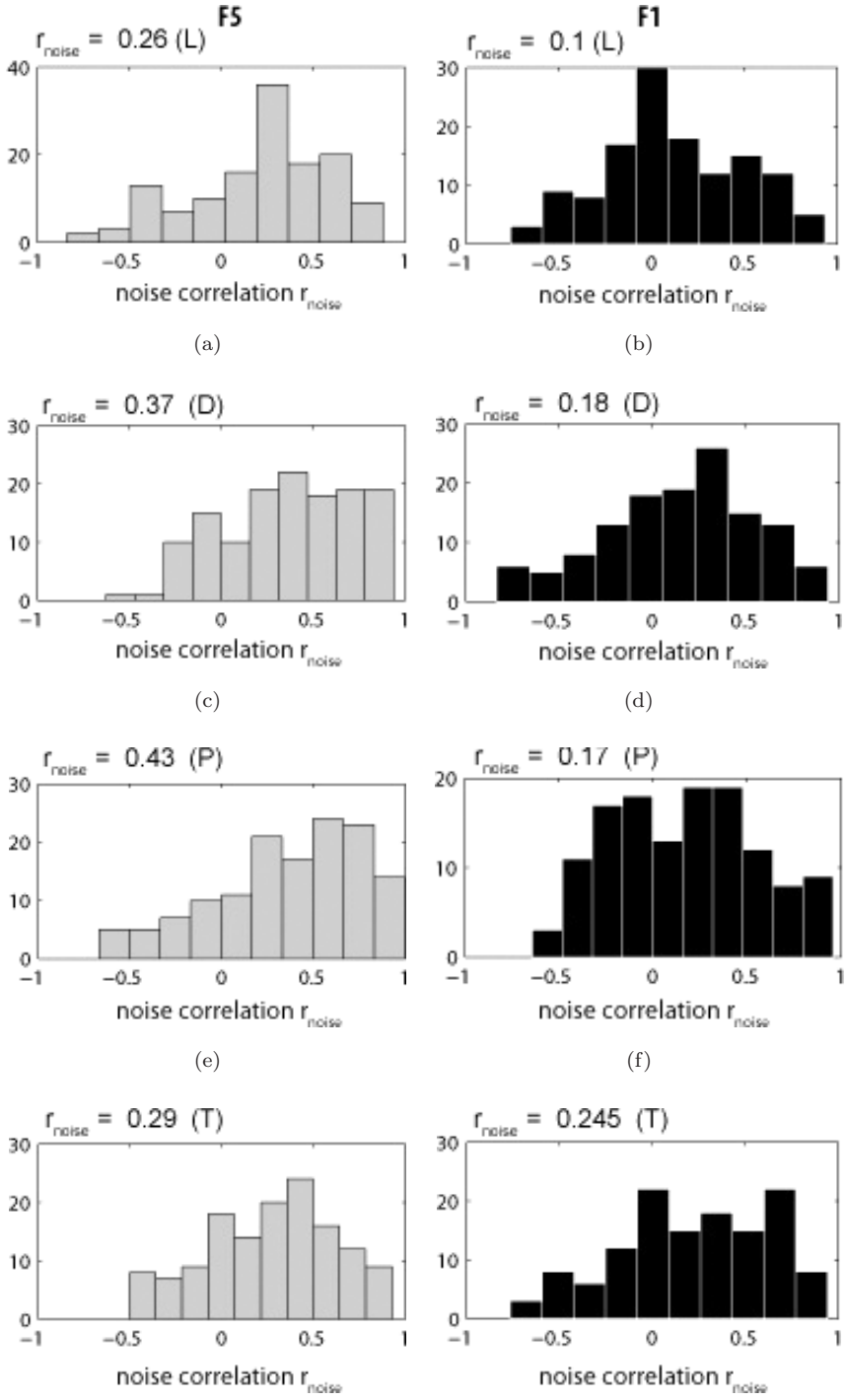

Fig. 9. Relationship between spike counts and r_{noise}, We consider the four stimulus that drove the pairs effectively. (a), (c), (e) and (g): population histograms of r_{noise} in area F5 (± 200 ms before and after 1 s) for **L, D, P** and **T** conditions, respectively. (b), (d), (f) and (h): population histograms of r_{noise} in area F1 (± 200 ms before and after 1 s) for **L, D, P** and **T** conditions, respectively. Forty-two pairs of neurons in F5 and thirty-six pairs of neurons in F1 were considered. The number next to each plot indicated by r_{noise} is the mean of the distribution.

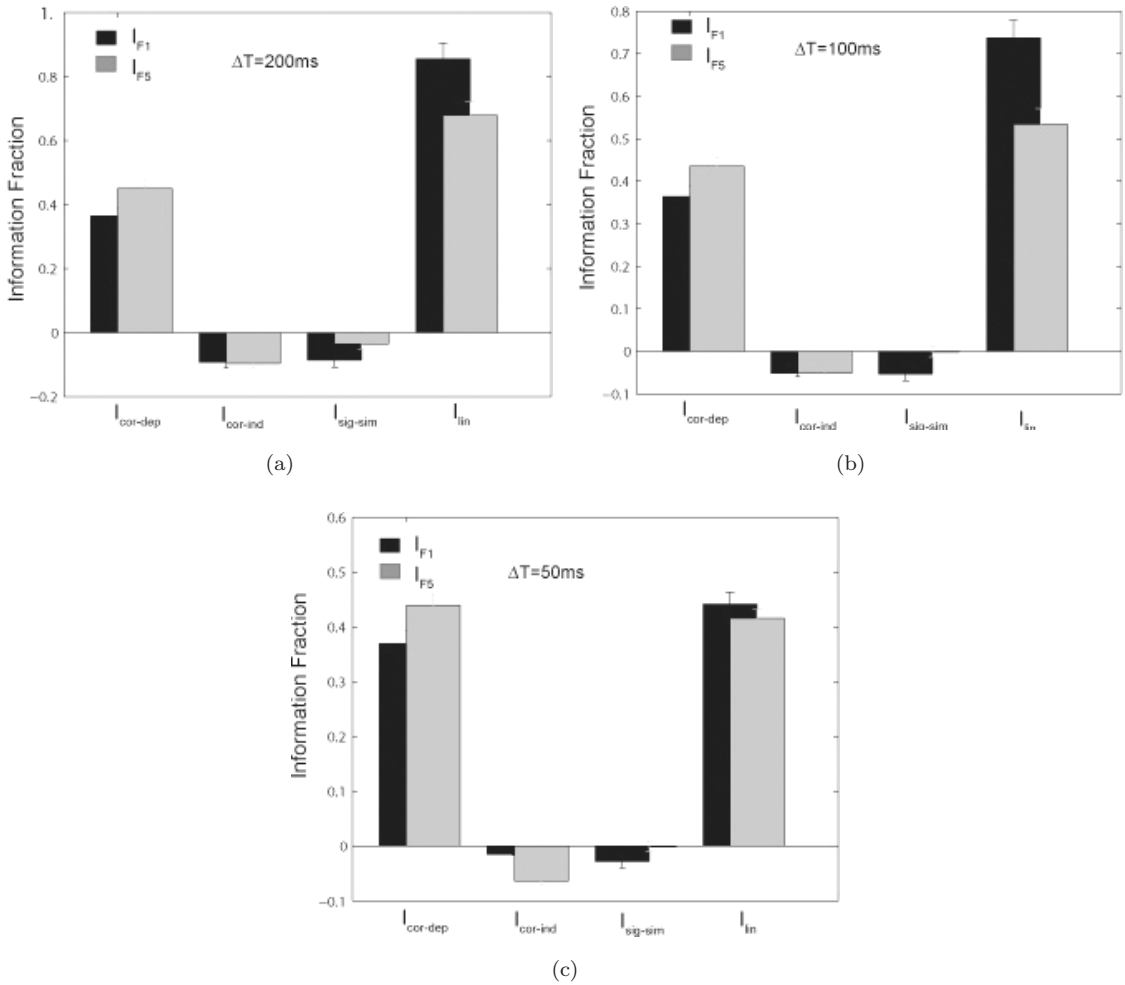

Fig. 10. Fraction of information components across the entire population of neurons. Forty-two pairs of neurons in F5 and 36 pairs of neurons in F1 were included. In the figures (a), (b), and (c) we considered two bins of ±200 ms, ±100 ms, and ±50 ms, respectively, before and after 1 s. Error bars indicate the standard deviation of the mean. The bar charts on the left-hand side of the figure illustrate the effects of the stimulus-dependent synchronization component, $I_{\mathrm{cor-dep}}$, the bar charts that follow are the average level of correlation, $I_{\mathrm{cor-ind}}$, the signal similarity contribution, $I_{\mathrm{sig-sim}}$, and the linear component, I_{lin}. Note that redundancy contributions due to the signal similarity term are higher for F1 than for F5, and that the linear component I_{lin} is more informative for F1 than for F5. In other words, within the motor cortex, information across pairs of cells is summed linearly. This is not the case in F5, where information across pairs of cells is summed superlinearly.

of correlations. In practice, we obtained $P_{\mathrm{ind}}(\mathbf{r}\,|\,s)$ numerically by multiplying the marginal probability distributions.

In the information breakdown formalism, Eqs. (1)–(6), the presence of noise correlation (correlation in response variability for a fixed stimulus) is given by $P(\mathbf{r}\,|\,s) \neq P_{\mathrm{ind}}(\mathbf{r}\,|\,s)$. On the other hand, the signal correlations are indicated by $P(\mathbf{r}) \neq P_{\mathrm{ind}}(\mathbf{r})$.

We performed information estimations using 12 trials per condition using QE sampling procedure[54] (considering the same mean rates but no noise correlations; 42 pairs of F5 and 36 pairs of F1) taking into account a Poisson simulation of uncorrelated neurons. Figure 11(c) shows the mean values of the information breakdown analysis. Note that having no noise correlations implies $I_{\mathrm{cor-dep}} = 0$ and $I_{\mathrm{cor-ind}} = 0$ despite the reduced number of

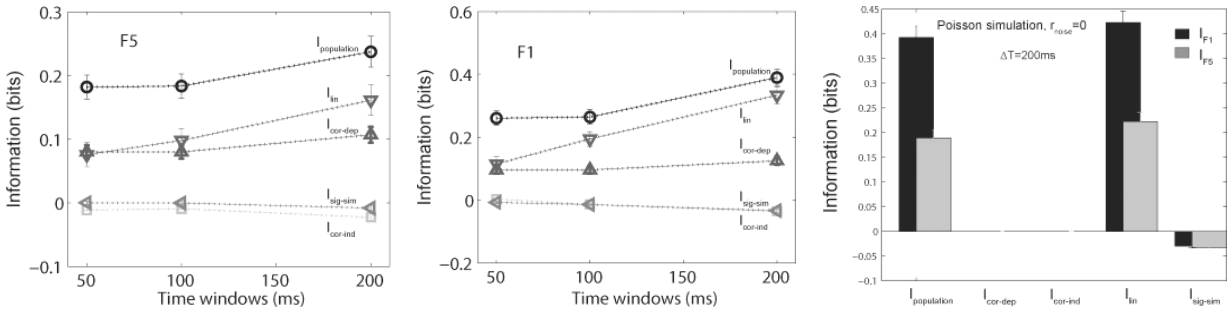

(a) (b) (c)

Fig. 11. The results of information breakdown analysis. (a) Information component analysis for F5 (average over 42 pairs of neurons), showing how the balance between a synergistic contribution attributable to the stimulus-dependent synchronization ($I_{\mathrm{cor-dep}}$) and redundant contributions from tuning overlap ($I_{\mathrm{sig-sim}}$) and the average level of correlation ($I_{\mathrm{cor-ind}}$) gives rise to the overall level of synergy. The information components I_{lin}, $I_{\mathrm{sig-sim}}$, and I_{cor} combine to give the total information, I_{ensemble}. (b) The average of 36 pairs of cells in F1, which leads to a roughly independent neural code. (c) Poisson simulation of uncorrelated neurons that have exactly the same mean rates to each stimulus as the neuronal pair under consideration, but no noise correlations. Having no noise correlations leads to $I_{\mathrm{cor-dep}} = 0$ and $I_{\mathrm{cor-ind}} = 0$, and it was important to use an effective sampling procedure (QE, Ref. 54).

trials. This is in agreement with the idea that $I_{\mathrm{cor}} = I_{\mathrm{cor-dep}} + I_{\mathrm{cor-ind}}$ quantifies whether the presence of "noise correlation" could increase or decrease the information available in the neural responses. Thus, the absence of noise correlation leads to $I_{\mathrm{cor-dep}} = 0$ and $I_{\mathrm{cor-ind}} = 0$. In order to obtain such result, it was crucial to use an effective sampling procedure (QE, Ref. 54), to avoid the results being contaminated by residual bias.

The type of independence shown by this simulation corresponds to activity or response independence, which applies if spike trains were truly uncorrelated, i.e. $p(r \mid s) = p(r_1 \mid s)p(r_2 \mid s)$. Thus if we assume zero noise correlation ($\gamma(r \mid s) = 0$ or $r_{\mathrm{noise}} = 0$) the information breakdown formalism expressed by Eqs. (1)–(6) reveals that $I_{\mathrm{cor-ind}} = 0$ and $I_{\mathrm{cor-dep}} = 0$. That is, the results obtained by taking a Poisson simulation of uncorrelated neurons are supported by a closer analytical examination of the correlation components in the information breakdown formalism, Eqs. (5) and (6). Hence our information theoretical approach, in combination with the use of an effective sampling procedure (QE, Ref. 54), guarantees the robustness of our results obtained considering 42 pairs of neurons in F5 and 36 pairs of neurons in F1.

The stimulus dependency of individual neurons activity, within area F5 and F1, to the four different conditions of visual feedback during hand grasping has been established in Ref. 5. In order to investigate stimulus dependent synchronization across pairs of neurons we used a methodology similar to the one implemented in Ref. 38. More specifically, this dependence between responses and stimuli may take a number of forms: firing rate dependence, pairwise correlation dependence, etc. Information component breakdown methods allow us to quantify the effect of such dependencies on the mutual information and thus assess the different ways in which the correlations contribute to the neural code. If synergistic or redundant interactions between cells are observed, the information components reveal the mechanisms from which they arise.

We use a Poisson simulation of uncorrelated neurons that have exactly the same mean rates to each stimulus as the neuronal pairs under consideration, but with no noise correlations and the same number trials for each of the four experimental conditions. We explicitly show, using this simulation under similar conditions to the experimental ones presented here, that we would obtain zero stimulus dependent synchronization, $I_{\mathrm{cor-dep}} = 0$, and zero independent stimulus synchronization, $I_{\mathrm{cor-ind}} = 0$, if there were no noise correlations across the pairs of neurons. Moreover, the use of different metrics to assess the degree of pairwise correlations together with

the application of the quadratic extrapolation procedure to remove bias deviation at its source[54] on the components of our information breakdown reinforces the reliability of our findings.

4. Discussion

Various forms of interactions among cortical neurons, including firing synchrony and local oscillations, have been considered as the key to form high-level representations.[68–72] The contribution of correlated discharge has largely been dismissed as reflecting coding redundancy in a noisy system. In particular, a previous study of pair-wise spike synchrony[72] reported that an excess of synchrony in motor cortical neurons would lead to redundant information. However, spike correlations in response variability can yield additional information that is only provided by the neuronal ensemble.[71–73] Our findings show substantial stimulus-dependent correlation between pairs of neurons. In our study, the stimulus-dependent correlation component, $I_{\mathrm{cor-dep}}$, was large enough to outweigh redundant effects due to the average level of correlation ($I_{\mathrm{cor-ind}}$), leading to an overall synergistic effect of correlations. Our results suggest that there is a significant quantity of synchronous spikes between pairs of cells in both the premotor and motor cortex areas. In the case of F5, the stimulus-dependent correlation component, $I_{\mathrm{cor-dep}}$, is about 15% higher than in F1. Moreover, $I_{\mathrm{cor-dep}}$, is about 45% of the total (shuffled) information (I_{sh}) in F5, whereas in F1 the stimulus-dependent correlation component, $I_{\mathrm{cor-dep}}$, is smaller. $I_{\mathrm{cor-dep}}$ is about 32% of the total shuffled information (I_{sh}) in F1. The results are robust for the different time windows used in the analysis. There is a significant amount of synchrony in both areas, effectively providing additional information about the stimuli beyond the information yielded by the independent firing. In a sense, this is surprising, because it would appear to contradict the findings of Oram suggesting that motor neurons provides redundant information related to direction of arm movement.[72] Nevertheless, our analysis suggests that correlations in the trial-to-trial response variability are more likely to increase than to decrease information content. Thus, pair-wise synchronization can be seen as a requirement for performing the synergistic movement needed to achieve effective motor control of grasping.

Functional classification of cortical neurons has typically consisted of finding qualitatively different responses to simple stimuli. In contrast, our analysis has revealed that average mutual information values provided by individual cells across the population, considering stimuli combinations with or without full vision of the hand, enable us to classify cells without imposing a metric on the space of stimuli or responses. Thus, a simple comparison of total linear mutual information estimations of different stimulus combinations with (or without) full vision provides us with a functional classification of cells as belonging to either F5 or F1. Cells can be clustered in such a way that most of the diversity is captured by the total linear mutual information values of the clusters, rather than by individual cell responses within clusters.

Nevertheless, spike correlations across neurons may also affect the coding of sensory information, being a consequence of common input from other neurons. Correlations between nearby neurons might be expected since they are thought to share the same thalamic projections in the primary motor cortex.[74] Functional studies have also shown that a large diffuse portion of the primary motor cortex is activated when simple reaching movements are made, thereby suggesting that the motor cortex is not organized as a set of independent columns, and correlations between the responses of neurons can encode information redundantly, independently, or synergistically.[67] If we consider a pair of neurons with overlapping tuning, and without stimulus-dependent correlation, the covariance of neuronal firing would limit the information carried by the neuronal population overall, due to the introduction of redundancy.[75]

As neural integration is usually understood as the algebraic representation and summation of excitatory or inhibitory postsynaptic potentials, which govern the potential for firing in the postsynaptic neuron, synchronization of presynaptic inputs can be thought of as a mechanism of neural integration. Moreover, at a fine temporal scale appears to be a natural mechanism for coordination and integration of neuronal activity, as shown by our current findings.

One of the goals of the current study was to address how synchronization of spike trains affects the neural coding of grasping, using four different

stimulus conditions. Our information component breakdown analysis illustrates the interplay of synergy from the stimulus-dependent component and redundancy from the average level of correlation, giving rise to a synergistic coding of correlations. The picture over the population of neuron pairs in F5 is one of a very significant amount of synergy, while information across pairs of cells in F1 is largely independent. This is consistent with the general picture shown by single-cell populations: the linear information conveyed by F1 is greater than the information conveyed by F5. However, we found that synchrony within the premotor and motor areas is prevalent, the pair-wise coding of grasping being more informative in F5 than in F1. So what is the use of spike synchronization? According to von der Malsburg, the binding of features belonging to one object is represented by synchronous neural discharges. Moreover, temporal correlations at fine scales could underlie aspects of a higher cognitive process such as binding, motor coordination, or even consciousness, because they could signal relationships between neurons carrying separate codes in their coarse temporal response measures.[75–77]

We found that the synergistic effects provided by pair-wise spike correlations across neurons in F1 are less than half of those noted for F5. Thus, information transmission across pairs of cells in F1 is largely independent, whereas information transmission across pairs of cells in the premotor cortex area F5 is summed superlinearly. These findings support the hypothesis that visual feedback information about the monkey's hand movement during the execution of a grasping task is accessible to the primary motor cortex through premotor cortical areas (as shown in Ref. 5). More importantly, we have shown here that the main mechanism of neuron–neuron communication lies at the level of the correlation code, rather than at the spike rate modulation. The brain, therefore, could take advantage of both the accuracy provided by independence in F1 and the synergy provided by the superlinear information population code of F5. This suggests that pair-wise interactions between neurons help to transform internal representations of visuomotor information into specific motor commands throughout the grasping. Thus, pair-wise synchronization could be seen as a requirement for performing the synergistic movement needed to achieve the effective motor control of grasping.

A final point should be made to consider a more general functional significance of this result. The motor system is a hierarchical structure, where upstream elements (and F5 is upstream to F1) are more and more capable of merging and generalization.[5] The generalizing role of F5 clearly emerges from the functional properties of its neurons. For example, neurons specifically discharging during precision grip performed with the right hand (but not during whole hand prehension) discharge also during the same type of grasping executed with the contralateral hand or, in fewer cases, even with the mouth. In addition, F4 neurons fire during arm movements to the mouth, while F5 neurons fire when the animal grasps objects with the hand and sometimes when it grasps objects with the mouth.[78] This means they generalize the concept of 'taking possession of a small object'.[5] The picture is completely different in area F1, where its proximity to the output and, in some cases, direct cortico-motoneuronal projections, more strictly link neurons to muscles. Our findings might also apply also to both ventral and dorsal sectors of premotor cortices. It is possible that the superlinear summation evidence shown by the present work is a neural correlate of the diverse roles played by the two areas within this hierarchical structure.

It has been hypothesized that Broca's area could derive phylogenetically from F5 premotor area of monkey where neurons involved in commanding grasp with hands and mouth and in recognizing grasp motor acts were recorded.[79,80] In humans it has been proved that the inferior parietal lobe has a major in integrating converging multimodal sensory information for coding of general action patterns (during real and imagined mouth grasping).[81] Our results provide deeper insights of how information is processed pre-motor and motor cortex area. In addition, these findings might have also implications for cognitive recovery and rehabilitation after brain injury.

Moreover, one main challenge in computational neuroscience is to provide an efficient algorithm of brian–computer interface (BCI) that could translate the recorded neural activity into a control signal for an external device.[82–90] The signal acquisition component is generally divided intotwo categories:

noninvasive and invasive.[91] There are a big variety of signal processing techniques such as time-frequency methods, spatiotemporal techniques, signal feature classification algorithms as artificial spiking neural networks, population coding, code specificity, information theoretical approaches, wavelet transform, etc., that can be used for discovering features and markers to be translated into desired actions.[41,91–94] Importantly, BCI technology is evolving to provide therapeutic benefits by inducing cortical reorganization via neuronal plasticity.[95] In that respect, it has been shown recently that cooperation between reticulospinal and corticospinal systems could provide insight for development of better rehabilitation approaches for stroke patients and others with movement disorders.[96] To some extent a successful BCI algorithm should also account for generalizing role of F5, as superlinear summation across neurons in this area help to transform internal representations of visuomotor information into specific motor commands throughout the grasping.

Acknowledgments

FM is Associate member of the National Research Career of CONICET Argentina. We gratefully acknowledge PIP 11220130100327CO (2014/2016) CONICET, Argentina (FM), RobotCub (Robotic Open-Architecture Technology for Cognition, Understanding and Behavior), IST-004370, the BMI Project of the RBCS Department at the Italian Institute of Technology, MIUR (PRIUN 2012) Grant to LF.

Appendix A

Figure A.1 presents a visual explanation of how the total mutual information is separated into components reflecting the contributions of individual coding mechanisms. $I(\mathrm{R};\mathrm{S})$ is the total (ensemble) mutual information. I_{lin} is the information that would be obtained if each neuron would to convey independent information. $I_{\mathrm{sig-sim}}$ corresponds to the signal similarity term which is a pure redundant contribution due to overlapping in the tuning cells. I_{cor} is the overall effect of synchronized firing, $I_{\mathrm{cor-ind}}$ is the effect of average level of correlation over stimuli. $I_{\mathrm{cor-dep}}$ is the contribution of the stimulus dependent synchronization.

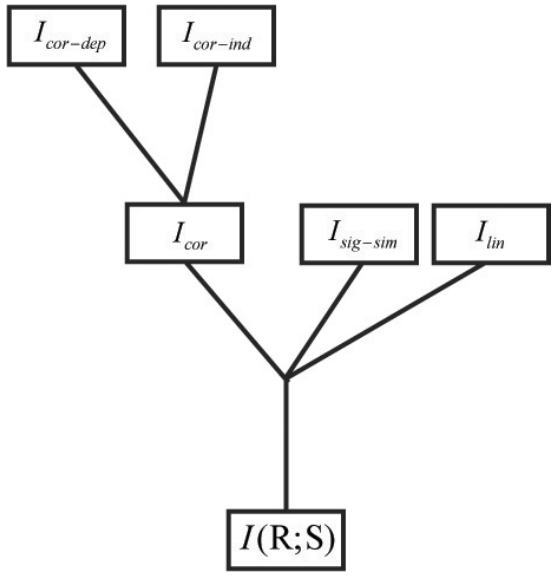

Fig. A.1. Information component breakdown. The ensemble mutual information can be broken down into a linear component, the reduction of information attributable to the redundancy caused by overlap in tuning curves, $I_{\mathrm{sig-sim}}$, and the contribution of synchronized firing $I_{\mathrm{cor}} = I_{\mathrm{cor-ind}} + I_{\mathrm{cor-dep}}$.

References

1. U. Castiello, The neuroscience of grasping, *Nat. Rev. Neurosci.* **6**(9) (2005) 726–736.
2. E. Olivier *et al.*, Precision grasping in humans: From motor control to cognition, *Curr. Opin. Neurobiol.* **17**(6) (2007) 644–648.
3. G. Rizzolatti *et al.*, Premotor cortex and the recognition of motor actions, *Brain Res. Cogn. Brain Res.* **3**(2) (1996) 131–141.
4. M. Jeannerod, M. A. Arbib, G. Rizzolatti and H. Sakata, Grasping objects: The cortical mechanisms of visuomotor transformation, *Trends Neurosci.* **18**(7) (1995) 314–320.
5. L. Fadiga, L. Caselli, L. Craighero, B. Gesierich, A. Oliynyk, B. Tia and R. Viaro, Activity in ventral premotor cortex is modulated by vision of own hand in action, *PeerJ* **1** (2013) e88,http://dx.doi.org.secure.sci-hub.org/ 10.7717/peerj.88.
6. L. Fogassi *et al.*, Cortical mechanism for the visual guidance of hand grasping movements in the monkey: A reversible inactivation study, *Brain* **124**(Pt 3) (2001) 571–586.
7. D. A. Nowak and J. Hermsdörfer, *Sensorimotor Control of Grasping*: *Physiology and Pathophysiology* (Cambridge University Press, Cambridge, New York, 2009), xiv, p. 509.
8. W. Gerstner and W. M. Kistler, *Spiking Neuron Models*: *Single Neurons*, *Populations*, *Plasticity*

(Cambridge University Press, Cambridge, UK, New York, 2002), p. 480.
9. F. Ponulak and A. Kasinski, Introduction to spiking neural networks: Information processing, learning and applications, *Acta Neurobiol. Exp.* (*Wars*), **71**(4) (2011) 409–433.
10. R. Brette, Computing with neural synchrony, *PLoS Comput. Biol.* **8**(6) (2012) e1002561.
11. F. Grammont and A. Riehle, Spike synchronization and firing rate in a population of motor cortical neurons in relation to movement direction and reaction time, *Biol. Cybern.* **88**(5) (2003) 360–373.
12. C. L. Witham, M. Wang and S. N. Baker, Cells in somatosensory areas show synchrony with beta oscillations in monkey motor cortex, *Eur. J. Neurosci.* **26**(9) (2007) 2677–2686.
13. F. Aboitiz, D. Cosmelli and SpringerLink (Online service), *From Attention to Goal-Directed Behavior Neurodynamical*, *Methodological*, *Clinical Trends* (Springer, Berlin, 2009), xvii, p. 327.
14. M. Ahmadlou and H. Adeli, Wavelet-synchronization methodology: A new approach for EEG-based diagnosis of ADHD, *Clin. EEG Neurosci.* **41** (2010) 1–10.
15. M. Ahmadlou and H. Adeli, Fuzzy synchronization likelihood with application to attention-deficit/hyperactivity disorder, *Clin. EEG Neurosci.* **42** (2011) 6–13.
16. M. Ahmadlou and H. Adeli, Visibility graph similarity: A new measure of generalized synchronization in coupled dynamic systems, *Physica D*, *Nonlinear Phenom.* **241** (2012) 326–332.
17. M. Ahmadlou, H. Adeli and A. Adeli, Fuzzy synchronization likelihood-wavelet methodology for diagnosis of autism spectrum disorder, *J. Neurosci. Methods* **211** (2012) 203–209.
18. R. Coullaut, I. Arbaiza, R. Bajo, R. Arrúe, M. E. Lopez, J. Coullaut-Valera, A. Correas, D. Lopez-Sanz, F. Maestu and D. Papo, Drug polyconsumption is associated with hypersynchronized brain activity at rest and in a counting task, *Int. J. Neural Syst.* **24** (2014) 1450005.
19. L. Wang, P. J. Liang, P. M. Zhang and Y. H. Qiu, Adaptation-dependent synchronization transitions and burst generations in electrically coupled neural networks, *Int. J. Neural Syst.* **24** (2014) 1450033.
20. M. Bandarabadi, J. Rasekhi, C. A. Teixeira, T. I. Netoff, K. K. Parhi and A. Douardo, Early seizure detection using neuronal potential similarity: A generalized low-complexity and robust measure, *Int. J. Neural Syst.* **25**(5) (2015) 1550019.
21. M. Chiappalone, A. Vato, L. Berdondini, M. Koudelka-Hep and S. Martinoia, Network dynamics and synchronous activity in cultured cortical neurons, *Int. J. Neural Syst.* **17**(2) (2007) 87–103.
22. A. Kohn and M. A. Smith, Stimulus dependence of neuronal correlation in primary visual cortex of the macaque, *J. Neurosci.* **25**(14) (2005) 3661–3673.
23. B. Strack, K. M. Jacobs and K. J. Cios, Simulating vertical and horizontal inhibition with short term dynamics in a multi-column, multi-layer model of neocortex, *Int. J. Neural Syst.* **24** (2014) 1440002.
24. G. Zhang, H. Rong, F. Neri and M. J. Perez-Jimenez, An optimization spiking neural P system for approximately solving combinatorial optimization problems, *Int. J. Neural Syst.* **24** (2014) 1–16.
25. S. Ghosh-Dastidar and H. Adeli, A new supervised learning algorithm for multiple spiking neural networks with application in epilepsy and seizure detection, *Neural Netw.* **22** (2009) 1419–1431.
26. S. Ghosh-Dastidar and H. Adeli, Improved spiking neural networks for EEG classification and epilepsy and seizure detection, *Integr. Comput. Aided Eng.* **14** (2009) 187–212.
27. A. Jahangiri and M. Durand, Phase resetting analysis of high potassium epileptiform activity in CA3 region of the rat hippocampus, *Int. J. Neural Syst.* **21**(2) (2011) 127–138.
28. J. L.Rosselló, V. Canals, A. Oliver and A. S. Morro, Studying the role of synchronized and chaotic spiking neural ensembles in neural information processing, *Int. J. Neural Syst.* **24**(5) (2014) 1430003.
29. S. Schliebs, N. Kasabov and M. Defoin-Platel, On the probabilistic optimization of spiking neural networks, *Int. J. Neural Syst.* **20**(6) (2010) 481–500.
30. G. Zhang, H. Rong, F. Neri and M. J. Pérez-Jiménez, An optimization spiking neural P system for approximately solving combinatorial optimization problems, *Int. J. Neural Syst.* **24**(5) (2014) 1440006.
31. J. Friedrich, R. Urbanczik and W. Senn, Code-specific learning rules improve action selection by populations of spiking neurons, *Int. J. Neural Syst.* **24**(5) (2014) 1450002.
32. P. Mesejo and O. Ibanez, E. Fernandez-Blanco, F. Cedron, A. Pazos and A. B. Porto-Pazos, Artificial neuron-glia networks learning paradigm based on cooperative coevolution, *Int. J. Neural Syst.* **25**(4) (2015) 1550012.
33. Z. Wang, L. Guo and M. Adjouadi, A generalized leaky integrate-and-fire neuron model with fast implementation method, *Int. J. Neural Syst.* **24**(5) (2014) 1440004.
34. S. Shapero, M. Zhu, J. Hasler and C. Rozell, Optimal sparse approximation with integrate and fire neurons, *Int. J. Neural Syst.* **24**(5) (2014) 1440001.
35. A. Vidybida, Testing of information condensation in a model reverberating spiking neural network, *Int. J. Neural Syst.* **21**(3) (2011) 187–198.
36. S. Ghosh-Dastidar and H. Adeli, Spiking neural networks, *Int. J. Neural Syst.* **19**(4) (2009) 295–308.
37. F. Montani *et al.*, The impact of high-order interactions on the rate of synchronous discharge and information transmission in somatosensory cortex,

Philos. Trans. A Math. Phys. Eng. Sci. **367**(1901) (2009) 3297–3310.
38. F. Montani *et al.*, The role of correlations in direction and contrast coding in the primary visual cortex, *J. Neurosci.* **27**(9) (2007) 2338–2348.
39. S. Panzeri *et al.*, Correlations and the encoding of information in the nervous system, *Proc. Biol. Sci.* **266**(1423) (1999) 1001–1012.
40. G. Pola *et al.*, An exact method to quantify the information transmitted by different mechanisms of correlational coding, *Network* **14**(1) (2003) 35–60.
41. K. J. Friston, Another neural code?, *Neuroimage* **5** (1997) 213–220.
42. J. W. Pillow *et al.*, Spatio-temporal correlations and visual signalling in a complete neuronal population, *Nature* **454** (2008) 995–999.
43. G. Gruenert, K. Gizynski, G. Escuela, B. Ibrahim, J. Gorecki and P. Dittrich, Understanding networks of computing chemical droplet neurons based on information flow, *Int. J. Neural Syst.* **25**(7) (2015) 1450032.
44. S. Aydin, N. Arica, E. Ergul and O. Tan, Classification of obsessive compulsive disorder by EEG complexity and hemispheric dependency measurements, *Int. J. Neural Syst.* **25**(3) (2015) 1550010.
45. F. C. Morabito, M. Campolo, D. Labate, G. Morabito, L. Bonanno, A. Bramanti, S. de Salvo, A. Marra and P. Bramanti, A longitudinal EEG study of Alzheimer's disease progression based on a complex network approach, *Int. J. Neural Syst.* **25**(2) (2015) 1550005.
46. A. Ortiz-Rosario, H. Adeli and J. A Buford, Wavelet methodology to improve single unit isolation in primary motor cortex cells, *J. Neurosci. Methods* **246** (2015) 106–118.
47. H. Hojjat and S. L. Hung, *Machine Learning*: *Neural Networks*, *Genetic Algorithms*, *and Fuzzy Systems* (John Wiley and Sons, NY, 1995).
48. A. Oliynyk, C. Bonifazzi, F. Montani and L. Fadiga, Automatic online spike sorting with singular value decomposition and fuzzy C-mean clustering, *BMC Neurosci.* **13** (2012) 96.
49. N. Schmitzer-Torbert, J. Jackson, D. Henze, K. Harris and A. D. Redish, Quantitative measures of cluster quality for use in extracellular recordings, *Neurosci.* **131**(1) (2005) 1–11.
50. T. M. Cover and J. A. Thomas, *Elements of Information Theory* (Wiley, 2006), p. 748.
51. S. Panzeri and S. R. Schultz, A unified approach to the study of temporal, correlational, and rate coding, *Neural. Comput.* **13**(6) (2001) 1311–1349.
52. S. Panzeri *et al.*, Correcting for the sampling bias problem in spike train information measures, *J. Neurophysiol.* **98**(3) (2007) 1064–1072.
53. A. Borst and F. E. Theunissen, Information theory and neural coding, *Nat. Neurosci.* **2**(11) (1999) 947–957.
54. S. P. Strong, R. Koberle, R. R. de Ruyter van Steveninck and W. Bialek, Entropy and information in neural spike trains, *Phys. Rev. Lett.* **80** (1998) 197–200.
55. A. Panzeri and A. Treves, Analytical estimates of limited sampling biases in different information measures, *Network* **7** (1996) 87–107.
56. M. A. Montemurro, R. Senatore and S. Panzeri, Tight data-robust bounds to mutual information combining shuffling and model selection techniques, *Neural Comput.* **19**(11) (2007) 2913–2957.
57. J. J. Eggermont, Neural interactions in cat primary auditory cortex II: Effects of sound stimulation, *J. Neurophysiol.* **71** (1994) 246–270.
58. D. H. Perkel, G. L. Gerstein and G. P. Moore, Neuronal spike trains and stochastic point processes. II: Simultaneous spike trains, *Biophys. J.* **7**(4) (1967) 419–440.
59. W. Bair, E. Zohary and W. T. Newsome, Correlated firing in macaque visual area MT: Time scales and relationship to behavior, *J. Neurosci.* **21**(5) (2001) 1676–1697.
60. A. Murata *et al.*, Selectivity for the shape, size, and orientation of objects for grasping in neurons of monkey parietal area AIP, *J. Neurophysiol.* **83**(5) (2000) 2580–2601.
61. H. H. Ehrsson, C. Spence and R. E. Passingham, That's my hand! Activity in premotor cortex reflects feeling of ownership of a limb, *Science* **305**(5685) (2004) 875–877.
62. M. A. Umilta *et al.*, Simultaneous recording of macaque premotor and primary motor cortex neuronal populations reveals different functional contributions to visuomotor grasp, *J. Neurophysiol.* **98**(1) (2007) 488–501.
63. R. B. Muir and R. N. Lemon, Corticospinal neurons with a special role in precision grip, *Brain Res.* **261**(2) (1983) 312–316.
64. R. Porter and R. Lemon, *Corticospinal Function and Voluntary Movement*, Monographs of the Physiological Society (Oxford University Press, Oxford, New York, 1993), xviii, p. 428.
65. C. von der Malsburg, *The Correlation Theory of Brain Function*, Internal Report, Max-Planck-Institute for Biophysical Chemistry, Department of Neurobiology, Göttingen, Vol. 81 (1981) p. 38.
66. L. F. Abbott and P. Dayan, The effect of correlated variability on the accuracy of a population code, *Neural Comput.* **11**(1) (1999) 91–101.
67. T. J. Gawne and B. J. Richmond, How independent are the messages carried by adjacent inferior temporal cortical neurons? *J. Neurosci.* **13**(7) (1993) 2758–2771.
68. W. Singer and C. M. Gray, Visual feature integration and the temporal correlation hypothesis, *Annu. Rev. Neurosci.* **18** (1995) 555–586.

69. E. Vaadia *et al.*, Dynamics of neuronal interactions in monkey cortex in relation to behavioural events, *Nature* **373**(6514) (1995) 515–518.
70. R. C. deCharms and M. M. Merzenich, Primary cortical representation of sounds by the coordination of action-potential timing, *Nature* **381**(6583) (1996) 610–613.
71. N. G. Hatsopoulos *et al.*, Information about movement direction obtained from synchronous activity of motor cortical neurons, *Proc. Natl. Acad. Sci. USA* **95**(26) (1998) 15706–15711.
72. M. W. Oram *et al.*, Excess synchrony in motor cortical neurons provides redundant direction information with that from coarse temporal measures, *J. Neurophysiol.* **86**(4) (2001) 1700–1716.
73. E. Stark *et al.*, Correlations between groups of premotor neurons carry information about prehension, *J. Neurosci.* **28**(42) (2008) 10618–10630.
74. Y. Shinoda and S. Kakei, Distribution of terminals of thalamocortical fibers originating from the ventrolateral nucleus of the cat thalamus, *Neurosci. Lett.* **96**(2) (1989) 163–167.
75. E. Zohary, M. N. Shadlen and W. T. Newsome, Correlated neuronal discharge rate and its implications for psychophysical performance, *Nature* **370**(6485) (1994) 140–143.
76. C. von der Malsburg and W. Schneider, A neural cocktail-party processor, *Biol. Cybern.* **54**(1) (1986) 29–40.
77. C. von der Malsburg, Binding in models of perception and brain function, *Curr. Opin. Neurobiol.* **5**(4) (1995) 520–526.
78. U. Castiello, Arm and mouth coordination during the eating action in humans, *Exp. Brain Res.* **115** (1997) 552–556.
79. G. Rizzolatti and M. A. Arbib, Language within our grasp, *Trends Neurosci.* **21** (1998) 188–194.
80. M. Gentilucci, F. Benuzzi, M. Gangitano and S. Grimaldi, Grasp with hand and mouth: A kinematic study on healthy subjects, *J. Neurophysiol.* **4** (2001) 1685–1699.
81. U. Castiello, K. M. B. Bennett, G. E. Egan, H. J. Tochon-Danguy, A. Kritikos and J. Dunai, Human inferior parietal cortex 'Programs' the action class of grasping, *J. Cogn. Syst. Res.* **1** (2000) 89–97.
82. Y. Zhang, G. Zhou, J. Jin, Q. Zhao, X. Wang and A. Cichocki, Aggregation of sparse linear discriminant analyses for event-related potential classification in brain–computer interface, *Int. J. Neural Syst.* **24**(1) (2014) 1450003.
83. J. Li, H. Ji, L. Cao, D. Zang, R. Gu and B. Xia, Evaluation and application of a hybrid brain computer interface for real wheelchair control with multi-degrees of freedom, *Int. J. Neural Syst.* **24**(4) (2014) 1450014.
84. Y. Zhang, G. Zhou, J. Jin, X. Wang and A. Cichocki, Frequency recognition in SSVEP-based BCI using multiset canonical correlation analysis, *Int. J. Neural Syst.* **24**(4) (2014) 1450013.
85. M. Nakanishi, Y. Wang, Y. T. Wang, Y. Mitsukura and T. P. Jung, A high-speed brain speller using steady-state visual evoked potentials, *Int. J. Neural Syst.* **24**(6) (2014) 1450019.
86. J. Jin, B. Z. Allison, Y. Zhang, X. Wang and A. Cichocki, An ERP-based BCI using an oddball paradigm with different faces and reduced errors in critical functions, *Int. J. Neural Syst.* **24**(8) (2014) 1450027.
87. J. Jin, E. W. Sellers, S. Zhou, Y. Zhang, X. Wang and A. Cichocki, A P300 brain computer interface based on a modification of the mismatch negativity paradigm, *Int. J. Neural Syst.* **25**(3) (2015) 1550011.
88. Y. Liu, Q. Zhao and L. Zhang, Uncorrelated multiway discriminant analysis of EEG motor imagery classification, *Int. J. Neural Syst.* **25**(4) (2015) 1550013.
89. D. Zhang, B. Huang, S. Li and W. Wu, An idle-state detection algorithm for SSVEP-based brain–computer interfaces using a maximum evoked response spatial filter, *Int. J. Neural Syst.* **25**(7) (2015) 1550030.
90. E. Yin, T. Zeyl, R. Saab, D. Huy, Z. Zhou and T. Chau, An auditory-tactile visual-saccade independent P300 brain-computer interface, *Int. J. Neural Syst.* **26**(1) (2015) 16500015.120.
91. A. Ortiz-Rosario and H. Adeli, Brain–Computer interface technologies: From signal to action, *Rev. Neurosci.* **24**(5) (2013) 537–552.
92. Y. Wang, J. C. Principe and J. C. Sanchez, Ascertaining neuron importance by information theoretical analysis in motor brain–machine interfaces, *Neural Netw.* **22**(5–6) (2009) 781–790.
93. M. Bongard, D. Micol and E. Fernandez, NEV2lkit: A new open source tool for handling neuronal event files from multi-electrode recordings, *Int. J. Neural Syst.* **24**(4) (2014) 1450009.
94. F. Su, J. Wang, B. Deng, X. L. Wei, Y. Y. Chen and H. Y. Li, Adaptive control of Parkinson's state based on a nonlinear computational model with unknown parameters, *Int. J. Neural Syst.* **25**(1) (2015) 1450030.
95. A. Burns, H. Adeli and J. A. Buford, Brain–Computer interface after nervous system injury, *The Neuroscientist* **20**(6) (2014) 639–651.
96. A. Ortiz-Rosario, I. Berrios-Torres, H. Adeli and J. A. Buford, Combined corticospinal and reticulospinal effects on upper limb muscles, *Neurosci. Lett.* **561** (2014) 30–34.